2005-09-02

Structure Elucidation of Bioactive Compounds Isolated from Endophytes of Alstonia scholaris and Acmena graveolens

Nicholas James Hundley
Brigham Young University - Provo

STRUCTURE ELUCIDATION OF BIOACTIVE COMPOUNDS ISOLATED FROM ENDOPHYTES OF ALSTONIA SCHOLARIS AND ACMENA GRAVEOLENS

by

Nicholas J. Hundley

A thesis submitted to the faculty of

Brigham Young University

in partial fulfillment of the requirements for the degree of

Master of Science

Department of Chemistry and Biochemistry

Brigham Young University

December 2005

BRIGHAM YOUNG UNIVERSITY

GRADUATE COMMITTEE APPROVAL

of a dissertation submitted by

Nicholas J. Hundley

This dissertation has been read by each member of the following graduate committee and by majority vote has been found to be satisfactory.

Date	Noel L. Owen, Chair
Date	Steven G. Wood
Date	Craig D. Thulin
Date	Barry M. Willardson

BRIGHAM YOUNG UNIVERSITY

As chair of the candidate's graduate committee, I have read the dissertation of Nicholas J. Hundley in its final form and have found that (1) its format, citations, and bibliographical style are consistent and acceptable and fulfill university and department style requirements; (2) its illustrative materials including figures, tables, and charts are in place; and (3) the final manuscript is satisfactory to the graduate committee and is ready for submission to the university library.

_____
Date

_____
Noel L. Owen
Chair, Graduate Committee

Accepted for the Department

_____
David V. Dearden
Graduate Coordinator

Accepted for the College

_____
Earl M. Woolley
Dean, College of Physical and Mathematical Sciences

ABSTRACT

STRUCTURE ELUCIDATION OF BIOACTIVE COMPOUNDS
ISOLATED FROM ENDOPHYTES OF
ALSTONIA SCHOLARIS AND
ACMENA GRAVEOLENS

Nicholas J. Hundley
Department of Chemistry and Biochemistry
Master of Science

Alstonia scholaris is an evergreen tree native to Southeast Asia and Australia. It is commonly used as a medicinal plant throughout these regions. In the present study, an endophyte of the genus *Xylaria* was isolated from a stem of *Alstonia scholaris*, its mycelia and exudate extracted, and the extract assayed for growth inhibition of HeLa cancer cells in vitro. Several known compounds were isolated and identified based on NMR, infrared, and mass spectral data. The compounds identified are 19,20-epoxycytochalasin C; 19,20-epoxycytochalasin D; and xylobovide. Two other compounds, fusaric acid and dehydrofusaric acid, were discovered in an endophyte of the Hypocreales family inhabiting the plant *Acmena Graveolens.*

ACKNOWLEDGMENTS

I would like to thank the many people who have helped me to complete this work. Special thanks goes to Dr. Noel Owen and Dr. Steven Wood who coached me through the process. I would also like to express my appreciation to Dr. Du Li for running the NMR samples, Bruce Jackson for the many sample runs on the mass spec machine, Dr. Allen Buskirk and Doug Tanner for help with all the little details of molecular handling, and Dr. Craig Thulin and Katie Southwick for assistance with the electrospray experiments. I am greatly indebted to all of them. I also express my thanks to the Department of Chemistry and Biochemistry for funding this research.

Table of Contents

1 Endophytes as Plant Symbionts: A Review [1]

1.1 Introduction

Virtually all plants are hosts to bacteria and fungi that can be classified as endophytes. Bacon et al. defines endophytes as "microbes that colonize living internal tissues of plants without causing any immediate, overt negative effects."[2] This particular definition implies a mutualistic relationship between the host plant and the endophytic microbe, whereas Strobel and colleagues suggest that the relationship can range from mutualistic to bordering on pathogenic.[3,4]

The most frequently encountered endophytes are fungi. It has been estimated that there may be over a million different fungal species on this Earth, of which only a small fraction (ca. 5%) have been identified.[5] There are also many bacteria that exist as plant endophytes, and indeed in most instances they coexist with endophytic fungi.

The existence of endophytes has been known for over one hundred years.[6] Botanists have carried out much research into the plant/endophyte relationship, especially for grasses such as tall fescue, where it has been shown that endophytes produce toxins that discourage insects and other grazing animals.[7] It wasn't until the past decade or so, however, that endophytes have been studied for their potential as novel sources of effective new drugs. Microbes, both fungal and bacterial, have provided modern medicine with valuable new cures, including penicillin from the fungus *Penicillium notatum*, and bacitracin from the bacterium *Bacillus subtilis*. Additionally, taxol, an important chemotherapeutic agent, is

synthesized by an endophyte of the Pacific Yew tree. Endophytes represent a huge diversity of microbial adaptations that have developed in special and sequestered environments, and their diversity and specialized habituation make them an exciting field of study in the search for new medicines. The hunt for new drugs is particularly important in view of the fact that so many diseases are developing resistance to some of the current treatments. This review will concentrate on what has been discovered, and what is still unknown about endophytes that synthesize chemicals with bioactive properties.

1.2 Current Knowledge about Endophytes

One of the early publications describing an endophytic fungus was by Freeman in 1904, and he makes reference to four other papers on endophytes that were published in 1898.[6] Freeman found the fungus in Persian darnel - an annual grass that today is considered a troublesome weed by many wheat farmers. In fact, grasses are probably the plants that have been most extensively studied as far as endophytes are concerned, and it was discovered that grasses with high endophyte content were often resistant to attack by certain insects.[8,9] In fact, darnel was apparently known to be toxic to some animals as far back as Roman times.[6] However considerable work has also been carried out on a variety of different plants,[2] including many trees and plants of horticultural importance (e.g. apple and kiwifruit.)[10] Analysis of any plant material may result in the discovery of a range of different endophytic fungi and bacteria (the actual numbers can range up to many tens), and several of the fungi would likely be specific to that particular host. Other than bacterial pathogens, there is no evidence that endophytic bacteria show the same host specificity.[11] This fungal-host specificity was found to be true for the fescue and rye grasses, where the endophytes

complete their life cycle within the above-ground portions of the grass host forming nonpathogenic, symbiotic associations.[11] In addition, environmental conditions such as soil, temperature and humidity etc., would also be expected to affect the nature and the population of endophytes.[12] It is not known if all endophytes synthesize bioactive metabolites, but the argument has been strongly made that those plants in unique environments that struggle to compete with other living organisms, or that need as much assistance as possible to survive, are likely to host endophytes which can generate secondary metabolites that will assist the plant.[13] Consequently, most investigations in search of novel metabolites have tended to concentrate on organisms that inhabit biotypes that represent unique survival challenges to plants, such as tropical forests, arid deserts and marine coral environments. Many scientists hold that plants growing in lush tropical rainforests, where competition for light and nutrients is severe, are most likely to host the greatest number of bio-active endophytes, and indeed a recent study noted that endophytes from tropical regions produced significantly more bio-active secondary metabolites than those from temperate parts of the world.[14] Interestingly, our own research findings appear to suggest that plants growing in arid desert regions may host as many bio-active endophytes as those collected in tropical forests. It is to be expected that even plants growing in cultivated gardens host endophytes.

1.3 The Plant/Endophyte relationship

The endophyte/host relationship is believed to be complex and variable from host to host and microbe to microbe. An early, in-depth analysis of an endophytic fungus in the plant *Helianthemum chamaecistus* by Boursnell, showed that in this instance the fungus passes from one generation to another through the seed.[15] The fungus enters the seedling

from the seed and spreads throughout the plant, entering new tissues as they arise. For this plant, germination and subsequent development of the seedling depends on the presence of the fungus; without it the plant ceases to grow beyond a certain stage. In addition, in the fall, the plant digests the swollen hyphae of the fungus that are found in the roots, and obviously benefits nutritionally from the microbe. The relation is truly mutualistic because the fungus must derive nourishment from the plant since it does not have contact with the soil. Similarly, endophytes that inhabit foraging grasses (e.g ryegrass) never leave their plant host and can only reproduce by invading seed tissue of the plant.[7]

On the other hand, fungi that reside solely in the mycorrhizae of a plant always enter from the soil, generally causing no damage to the root system.[16] Mycorrhizal fungi are generally thought to supply the host plant with inorganic resources from the soil while themselves gaining requisite nutrition from the plant.

Some research workers have suggested that in certain instances, the host/guest relationship may be more akin to a balanced pathogen-host antagonism than a truly synergistic one.[17] It has also been suggested that endophytic fungi might contribute to the process of nutrient recycling by initiating the biological degradation of the dying host plant.[4] There is some evidence that intercellular endophytes do elicit a chemical reaction from the host plant despite their largely benign relationship. For example, in douglas-fir seedlings, the plant produces the chemical resveratrol, which is a known anti-fungal agent, in response to endophyte infection.[18]

Endophytes, of course, can be involved in pathogenicity of host plants. The endophyte population in abnormally developed plant tissues, such as in galls and cysts, is often quite different from healthy sections.[19]

1.4 The Effects of Endophyte Colonization on Plant Survival

Many experiments have been conducted to compare how endophyte-infected plants and non-infected plants behave in relation to environmental stress and predation. Micorrhizal endophytes are known to be beneficial to the host plant by enhancing the absorption of soil nutrients such as phosphorus and other inorganic elements. Some mycorrhizal endophytes are known to be nitrogen-fixing entities, enabling plants such as Brazilian sugarcane to be cultivated for many years without the addition of nitrogen.[20]

In addition, it is has been shown that the colonization of micorrhizal fungi increases water flow through plants, in both agronomic and arid land.[21] The mechanism for this is still under discussion, but it is suggested that endophyte-infected plants often have larger root systems than non-infected hosts. Roots of endophyte-infected plants are found to be smaller in diameter, but with longer root hairs compared with non-infected variety, resulting in increased root surface area. This in turn can lead to enhanced water acquisition and affect the water-holding properties of the soil.[22] In fact, mycorrhizal colonization can effect a delay in flowering and longer retention of leaves, thus allowing the plant to secure a greater amount of carbon. It has also been suggested that endophytes increase water flow through plants by producing water-soluble chemicals such as alkaloids that act to increase osmotic flow through the roots.[23] Others have shown that endophyte infection affects the concentration of abscisic acid in leaves of drought-stressed grasses, and have suggested that this compound helps the recovery of endophyte-infected plants in water-deficient situations.[24] In addition, there is little doubt that micorrhizal fungi provide protection against soil pathogens, and since more than one fungus can occupy a root system, endophyte-

infected plants may benefit from the presence of several fungi, each of which may contribute differently to the well-being of the host.

Endophytes that reside in leaves and stems of plants also contribute to the host's successful survival. The array of alkaloids and other chemicals synthesized by the endophytes endow the plant with more resistance to nematodes, insects and livestock. It has also been suggested that the main advantage of endophyte infection to plants may be that endophytes are stimulated to increase production of chemical toxins after damage to the plant has occurred.[7] Interstingly, the presence of an endophyte in a perennial temperate grass such as tall fescue enables it to thrive outside of typical adaptation zones. For example, endophyte-infected tall fescue still grows and persists in the south eastern coastal plain of the USA, whereas non-infected material has apparently succumbed to stresses associated with the environment, such as water deficit, insects and nematodes, high temperatures and soil acidity.[25]

Orchids are among the many plants that host endophytic fungi. Orchid seeds are very small and may lack sufficient nutrients to sustain orchid embryo development. The endophytic fungus grows out of the seeds after dispersal and enzymatically degrades the bark and other substrates to supply nutrients for the developing orchid embryo.[19]

In summary, endophyte infection bestows considerable advantages to plants in terms of resistance to predators including pathogenic fungi, survival in drought situations, fecundity and general fitness. Indeed, plants endowed with specific endophytes are often able to grow faster due to the production of phytohormones and to become so competitive that they dominate in a particular environment.

For the endophyte the benefits of this symbiotic relationship have not been explored or analyzed to the same extent, but the plant host is able to supply the necessary nutrients and the compounds required for the endophyte to complete its life cycle. Unlike the plant host, many endophytes are able to survive under quite extreme and inhospitable conditions. In one study, hyphae within stored micorrhizal roots survived six years in dry soil, [16] and endophytes can be extracted from plant samples long after the plant tissue has died.

1.5 Some Important discoveries

A large number of secondary metabolites have been extracted, isolated and characterized from endophytic microbes, and these are detailed with extensive references in the reviews of Tan and Zou[26] and Strobel and colleagues.[4,13] Many of these compounds are bioactive, and the range includes alkaloids, steroids, terpenoids, peptides, polyketones, flavonoids, quinols and phenols as well as some chlorinated compounds.

Fungal metabolites from endophytes greatly affect the biology of predators. A number of experiments have been conducted by different research groups on the effect of endophyte infection of various grasses on insect and vertibrate herbivores.[7] Although results do tend to vary from plant to plant and from insect to insect, there is a correlation that strongly suggests that herbivores prefer to eat non-infected grasses and that avoiding infected grasses contributes to insect survival. For example, crickets restricted to infected ryegrass died within 48 hours, yet they survived when fed uninfected plants.[27] The issue of induced resistance to herbivores, as compared with constitutive resistance has also been investigated, and there is evidence that damage to leaf tissue does induce increased resistance to certain

herbivores. It has also been suggested that plant tissue damage caused by animal grazing tends to induce resistance to insect herbivores.[7]

The question of how microbial endophytes gain access to their host plants has also been the subject of study. Obviously most micorrhizal fungal endophytes and bacterial endophytes from the soil gain access through the roots, but bacterial endophytes are not thought to invade plant tissue directly; instead, they tend to enter the plant through natural openings or wounds.[28] Such openings may be in the root system or on aerial parts of the plant, and in some cases air-borne microbes can infect the fruit of a plant by entry through flowers.

The compound taxol (currently used as an anti-cancer agent) was first found in the bark of the Pacific yew tree. Later, it was discovered that a fungus associated with the yew tree also produces taxol.[29] Further analysis found that the genes for taxol production are found in both the tree and the fungus. It seems rather unlikely that this common ability evolved independently, and so the alternative explanation implies transfer of genetic information, either from the tree to the fungus or vice versa. Tan and Zou suggest the possibility that 'genetic recombination' of the endophyte with the host could occur over an evolutionary time period.[26]

Taxol has strong anti-fungal properties, and it has been proposed that its original purpose was as an anti-fungal agent to protect the plant (and the fungus) from other pathogenic fungi.[13] Since the original discovery of taxol in the bark of the North American Pacific yew tree (*Taxus brevifolia*), and its subsequent discovery in other *Taxus* species as well as in endophyte fungi associated with that tree species, taxol has been found to be

synthesized by endophytic fungi associated with other tree species (e.g. cypress, pine) growing on many different continents.[13]

Another interesting example of the protective power of an endophyte involves an aquatic plant *Rhyncholacis penicillata* from Venezuela. This plant grows in a river system where it is constantly buffeted against the rocks by the force of the water and floating debris. This situation should provide ample opportunity for pathogenic oomycetes (water molds) to enter the plant, but the plant population appeared quite healthy. Upon extracting and studying the endophytes from this host plant, Strobel and colleagues identified a potent anti-fungal bacterium, which was shown to produce oocydin A, a novel anti-oomycetous compound that obviously provided the plant with the requisite protection from the pathogenic microbes.[30]

A previously unknown compound showing significant bio-activity has been extracted and isolated from an endophytic fungus found in the leaves of a plant from the highlands of Papua New Guinea. The plant *Desmodium uncinatum* is used by the indigenous people for healing wounds and body sores. The compound shows anti-fungal and anti-bacterial effects and has been shown to destroy HeLa cervical cancer cells with an IC_{50} value of 0.9 μg/mL.[31]

Traditional medicines are extensively used in China, and there are over 5000 plants and plant products in their pharmacopeia. Work has already been initiated by Tan and others to investigate the endophytes in these plants.[26] For example, one Chinese plant that has become important in the treatment of malaria (*Artemisia annua*) also hosts endophytic fungi that produce several indole-based metabolites, some of which show activity against Gram-positive and Gram-negative bacteria and plant pathogenic fungi. Others behave as growth

promoting phytohormones.[32] Related fungi from another Artemisia species, *A. mongolica*, also produce anti-microbial metabolites.[33]

1.6 The Question of Communication

Plants are known to send chemical messages to call for assistance when they are attacked or when under stress. For example, Lima bean plants emit a chemical distress signal that attracts carnivorous mites if the plant is infested by spider mites. The latter are then devoured by the former. The signal apparently also inspires nearby uninfested lima bean plants to do the same thing.[35]

The possibility that not only the plants, but the microbes within them may communicate with each other is also quite plausible according to the research of Bassler.[34] She claims that various bacterial species use genetic or molecular mechanisms to communicate information that will allow the bacteria to work as a united entity. The fact that certain endophytes appear to be host-specific implies that they are very much aware of their immediate environment—a result that has been verified by experimentalists who have discovered that sometimes the production of bio-active compounds synthesized by an endophyte growing in culture outside the plant cell environment ceases after a specific time.[29] In the case of taxol, it was found that its production outside the plant could be increased by addition of several different chemicals, with benzoic acid being the most effective.[29] These findings suggest that more research into factors that can induce the formation of bio-active compounds might be valuable in the search for new medicines. Since fungi and bacteria coexist within plant hosts, and since it appears that endophytes are aware of their immediate environment, it follows that the two microbial species would be aware of

each other's presence. Consequently, it is not inconceivable that some communication may occur between them. From recent work in our laboratory, endophytic microbes showing anti-bacterial properties were extracted from a plant collected from the deserts of southern Utah. It was discovered that the active culture contained both a fungus and a bacterium. These were isolated and tested individually resulting in the discovery that although both showed approximately the same anti-bacterial activity, when placed together the bioactivity increased by a factor of three. It has not been determined whether communication, competition, or chemical synergy increased the toxicogenic properties of the endophytes.[31]

Communication between endophyte and host is implied in the conclusion expressed by Belesky and Malinowski that shoot-localized endophytes can induce changes in root morphology and root function. These changes may be a result of intricate signaling and bio-feedback systems involving the symbionts.[36] Findings such as these suggest that greater understanding of microbial communication may lead to methods of disrupting or enhancing this communication for the purpose of treating infectious diseases of both humans and plants.

1.7 The Study of Endophytic Organisms and their Metabolites

1.7.1 Isolation of Endophytes

In vivo discovery and identification of endophytic microbes is difficult; the endophyte/host relationship tends to be inconspicuous. The microbes reside within intercellular spaces of the tissues and possibly within the plant cells themselves. In this context, structural tools such as X-ray and electron diffraction are not very useful, and it

remains to be seen whether more specialized analytical methods can be developed that will enable scientists to successfully probe under the outer surface of a plant.

Traditionally, staining techniques (e.g. thionin/phenol) have been used so that fungal hyphae could be distinguished from the cell tissues.[15] More recently, once the plant samples (a leaf or stem or part of the root) have been collected, the endophytes are encouraged to leave the host and to grow upon Petri plates containing water agar, and later in nutrient-rich liquid media. Typically, small plant samples (leaves, stem or roots) are collected in the field, and stored in plastic bags (preferably cooled) for transportation to a laboratory. Although the plant sample may wither a little if in storage for more than a few days, the endophytes contained therein appear to be able survive without any obvious adverse effects for several weeks. Care must be taken, however, that entry of non-endophytic microorganisms into the dead plant sample does not occur.

In the laboratory, the plant surfaces are sterilized to remove all microbial epiphytes by soaking in 70% ethanol. Then, with a sterilized knife and in a laminar-flow hood, the outer tissues of the sample are cut so as to expose the interior surface to water agar on a covered culture plate. After about a week's incubation at room temperature, hyphal tips of fungi and bacterial growth can be seen exuding from the plant sample. Small cuts of these growths are then transferred onto new water agar plates or onto more nutrient-rich potato dextrose plates, and repetitive re-plating of the microbial colonies is continued until a pure culture is obtained. Differences in morphology, shape and color help to distinguish between different microbial entities. For bio-activity testing, obtaining a pure fungal or bacterial culture is not crucial at first, because in some instances greater activity is generated when endophytes stimulate and interact with each other.

1.7.2 Endophyte Identification

Endophytic fungi and bacteria can be identified most reliably using polymerase chain reaction (PCR) and DNA sequencing. PCR can be performed on cultured endophytes using primers that amplify DNA encoding ribosomal RNA. Identification of fungal endophytes can best be accomplished by amplification of Internal Transcribed Spacer (ITS) regions, which are repeating units of DNA encoding ribosomal RNA. These regions evolve rapidly and there is a very large database of sequences on Genbank and the AFTOL (Assembly of the Fungal Tree of Life) project. Another sequence that is sometimes useful in identification of fungal species is the 18S ribosomal DNA. There is less diversity in this sequence across species, especially among families, but in conjunction with ITS sequence data, 18S rDNA data can be helpful.

Since many of the fungi isolated from plants are likely to be novel, it is helpful to have primers covering as many taxonomic groups as possible. Primers specific to bacteria can also be used to identify bacteria. Sequencing the amplified DNA and comparing it with the database can help determine whether or not the specimen is novel; if the sequence is known, the species can be identified.

1.7.3 Isolation of Bioactive Compounds

Once endophytes are successfully cultured, bioassay-guided fractionation of growth media is used to isolate the most promising compounds. Here it must be stressed that having appropriate bio-assays available in order to check the activity of an endophyte is crucial to

the isolation and purification of the active components. The active microbial fungi are eventually transferred onto liquid media (M1D or potato dextrose broth) in large flasks, and allowed to grow for several weeks (Mueller Hinton broth tends to be better suited for bacteria). The liquid is filtered before being tested for bio-active compounds, and the compounds synthesized by the microbes are extracted from the liquid using various organic solvents. Isolation and purification of the bio-active compounds is attained through chromatographic techniques such as thin layer chromatography (TLC) and high pressure liquid chromatography (HPLC).

The type of bioassays used in this work depends largely on the interests of the investigators, but tests for anti-bacterial, anti-fungal and cytotoxic properties are easy to prepare and conduct.

1.7.4 Anti-bacterial assay

Two simple methods can be utilized for the testing of crude filtered growth media for anti-bacterial properties; the first is a paper disc method and the second involves a liquid assay. For the former, a bacterial "lawn" of fast-growing *Pseudomonas aeruginosa* is generated in a petri dish containing Mueller Hinton agar using sterile glass beads. Paper discs are then placed on this lawn and small aliquots of filter-sterilized endophyte growth media are pipetted onto the discs. Several different media samples can be run concurrently, and activity is determined by a visual zone of inhibition surrounding the discs.

The liquid anti-bacterial method involves adding the bacterium *Pseudomonas aeruginosa* in a broth to a 96-well plate and adding endophyte media at varying concentrations to the wells. Inhibition of growth in the wells is determined by optical transmittance through the wells.

1.7.5 Anti-fungal assay

Again there are two possible approaches to an anti-fungal assay. In a competitive assay, two fast-growing fungi (e.g. Pythium and Geotricium) are placed on opposite sides of a petri dish, and a plug containing a drop of the endophyte liquid is placed at the center of the plate. If the endophyte has any anti-fungal activity, the center spot will have a strong zone of inhibition surrounding it. In a non-competitive assay, the liquid extracted from the endophyte is placed in a 6-well plate containing M1D solution, and Geotricium or Pythium is added to the wells. The wells may be inspected at 24 hr intervals and the growth of the added fungus compared with that in a control medium.

1.7.6 Cytotoxicity assay

This assay measures the ability of the plant extract to inhibit the growth of cancer cells in vitro. Immortalized HeLa cervical cancer cells (or any other available cancer cells) can be used for this purpose. The cells are incubated for 24 hr in 96-well plates before the plant extract is added. Sulfurhodamine is added as a dye, and the color identifies living cells as opposed to those that have been killed by the extract. The same procedure can then be repeated using normal cells in order to compare the efficacy of the drug against cancer cells.

1.7.7 Structural studies

After obtaining a sample of pure bio-active material, the final goal is to determine its structure and composition. The two main structure-determining techniques used for this work are mass spectrometry (MS) and nuclear magnetic resonance spectroscopy (NMR). Both of these methods have seen vast improvements in sensitivity and technological advances over the past ten years, and when taken in tandem they represent very powerful

means of solving unknown molecular structures. In addition, X-ray diffraction is also available as a powerful method if the sample can be crystalized. High-resolution mass spectrometry can, in most instances, provide the molecular mass to such a precision that the molecular formula can also be determined. The exact number of hydrogen and carbon atoms can usually be verified from 1D NMR data, and various 1D and 2D experiments can give information about connectivities between magnetic nuclei in the sample, elucidating the full structure. It should be noted however that not all experiments lead to the discovery of a totally new chemical compound; occasionally the structural probing reveals a known bio-active chemical, although its source might be novel.

1.8 Future work and unanswered questions

This research field is in its infancy. Although many interesting and potentially valuable bio-active products synthesized by endophytes have been identified and characterized, there is much more to be discovered. In addition, there are many questions for which we have no answers currently, and which will need to be addressed before we can fully utilize the powerful synthetic potential of endophytic microbes. Historically, the study of endophytes has been the purview of botanists, but the recent discovery of interesting chemical compounds generated by certain endophytes has opened the field to structural chemists and biochemists. Real success in this area will probably only be achieved through an interdisciplinary approach, whereby the knowledge and insight of the botanist is combined with the technology and structural tools of the chemist.

1.9 References

(1) Owen, N.L. and Hundley, N.J. *Science Progress*. **2004**, 87 (2), 79-99.

(2) Bacon, C. W. and White, J. F. *Microbial Endophytes*, Marcel Dekker: New York, 2000.

(3) Petrini, O. Fungal endophytes of tree leaves. In *Microbial Ecology of Leaves*, Andrews, J. H. and Hirano, S. S. (eds) Springer-Verlag: New York, 1991, 179-187.

(4) Strobel, G. A. *Crit Rev Biotech*. **2002**, 22, 315-333.

(5) Hawksworth, D. L. and Rossman, A. Y. *Phytopath.* **1997**, 87, 888-891.

(6) Freeman, E.M. *Trans. Royal Soc. London (Biol)*, **1904**, 196, 1-27.

(7) Bultman, T. L. and Murphy, J. C. Do fungal endophytes mediate wound-induced resistance? In *Microbial Endophytes*, Bacon, C. W. and White, J. F. (eds) Marcel Dekker: New York, 2000, chapter 16, 421-452.

(8) Clay, K. *Ecology*, **1988**, 69, 10-16.

(9) Redlin, S. C. and Carris, L. M. *(*eds*) Endophytic Fungi in Grasses and Woody Plants: Systemics, Ecology and Evolution*, APS Press: St Paul, 1996.

(10) Pennycook, S. R. and Samuels, G. J. *Mycotaxon*, **1985**, 24, 445-458.

(11) Bacon, C. W. and De Battista, J. Endophytic fungi of grasses. In *Handbook of Applied Mycology, vol 1, Soil and Plants*. Arora, D. K., Rai, B., Mukerji, K. G. and Knudsen G. R. (eds), Marcel Dekker: New York, 1991, 231-356.

(12) Hata, K, Futai, K. and Tsuda, M. *Can. J. Bot*., **1998**, 76, 245-250.

(13) Strobel, G. A., Daisy, B., Castillo, U. and Harper, J. *J. Nat. Prod*., **2004**, 67, 257-268.

(14) Bills, G., Dombrowski, A., Pelaez, F., Polishook, J. and An, Z. Recent and future discoveries of pharmacologically active metabolites from tropical fungi. In *Tropical*

Mycology: Micromyceyes; Watling, R., Frankland, J. C., Ainsworth, A. M., Isaac, S. and Robinson, C. H. (eds) CABI Publishing: New York, 2002, vol 2, 165-194.

(15) Boursnell, J. G. *Annals of Botany*, **1950**, 14, 217-243.

(16) Kyde, M. M. and Gould, A. B. Mycorrhizal Endosymbiosis. In *Microbial Endophytes*, Bacon, C. W. and White, J. F. (eds) Marcel Dekker: New York, 2000, chapter 8, 161-198.

(17) Schultz, B., Rommert, A. -K., Dammann, U., Aust, H. -J., and Strack, D. *Mycol. Res.* 1999, 105, 1275-1283 .

(18) Sylvia, D. M. and Sinclair, W. A. *Phytopathology*. **1983**, 73, 390-397.

(19) Stone, J. K., Bacon, C. W. and White, J. F. An overview of endophytic microbes: endophytism defined. In *Microbial Endophytes,* Bacon, C. W. and White, J. F. (eds), Marcel Dekker: New York, 2000, chapter 1, 3-29.

(20) Boddey, R. M., Urquiaga, S., Reis, V. and Dobereiner, J. *Plant & Soil*, **1991**, 137, 111-117.

(21) Herman, P. Biodiversity and evolution in mycorrhizae of the desert. In *Microbial Endophytes*, Bacon, C. W. and White, J. F. (eds) Marcel Dekker: New York, 2000, chapter 7, 141-160.

(22) Schulze, E. -D. Water and nutrient interactions with plant water stress. In *Response of Plants to Multiple Stresses*, Mooney, H. A., Pell, E. J. and Roy, J. (eds) Academic Press: San Diego, 1991, 89-101.

(23) Bacon, C. W. *Agri. Ecosys. Env.* **1993**, 44, 123-141.

(24) Joost, R. E., Sharp, R. E. and Holder, T. L. Involvement of the Acremonium-endophyte in ABA-mediated gas exchange responses in tall fescue. Tall Fescue Toxicosis workshop, Atlanta, GA. *SERAIEG*, 1993, 8, 41-42.

(25) Bouton, J. H., Gates, R.N., Belesky, D. P. and Owsley, M. *Agron. Journal*, **1993**, 81, 220-223.

(26) Tan, R. X. and Zou, W. X. *Nat. Prod. Rep*. **2001**, 18, 448-459.

(27) Ahmad, S., Govindarajan, J. M., Funk, C. R. and Johnson-Cicalese, J. M. *Entom. exper. et appl.* **1985**, 39, 183-190.

(28) Huang, J. -S. *Ann. Rev. Phytopath.* **1986**, 24, 141-15728.

(29) Li, J.Y., Sidhu, R. S., Ford, E. J., Long, D. M., Hess, W. M. and Strobel, G.A. *J. Ind. Micro. & Biotech.* **1998**, 20, 259-264.

(30) Strobel, G. A., Li, J. Y., Sugawara, F., Koshino, H, Harper, J. and Hess, W. M. *Microbio.* **1999**, 145, 3557-3564.

(31) Owen N. L. et al. unpublished work.

(32) Lu, H., Zou, W. X., Meng, J. C., Hu, J. and Tan, R. X. *Plant Sci*. **2000**, 151, 67-73.

(33) Zou, W. X., Meng, J. C., Lu, H., Chen, G. X., Shi, G. X., Zhang, T. Y. and Tan, R. X. *J. Nat. Prod.* **2000**, 63, 1529-1530.

(34) Taga, M. E. and Bassler, B. L. *Proc. Natl. Acad. Sci.* **2003**, 100, 14549-14554.

(35) Achenbach, J. National Geographic, 2004, February, 205, 2, 1.

(36) Belesky, D. P. and Malinowski, D. P. Abiotic stresses and morphological plasticity and chemical adaptations of *Neotyphodium*-infected tall fescue plants. In *Microbial Endophytes*, Bacon, C. W. and White, J. F. (eds) Marcel Dekker: New York, 2000, chapter 17, 455-484.

2 Isolation of Fungal Secondary Metabolites from an Endophyte of Alstonia scholaris

2.1 Introduction

Alstonia scholaris is a tree native to Australia, New Guinea, Malaysia, and other parts of Southeast Asia. The plant produces milky cyanide-containing latex with abundant alkaloids. Common Australian names for the tree are Milkwood, Milk Bean, Milky Pine, and White Cheesewood. The plant is common in Queensland, where its bark was used by aborigines to treat abdominal pains, dysentery, and fevers. The milk was used for toothaches and neuralgia.[1]

A few leaves of Alstonia scholaris were collected in April 2003 at the Australian Canopy Crane Research Facility in the Daintree forest near Cairns in Queensland, Australia. The resident botanist at the facility identified the samples. The tissue samples were stored in plastic bags and sent to the United States where they were stored under refrigeration until culture on endophytes was performed in May 2003.

The endophytic fungus labelled 6/35 was selected for further investigation from a culture of the stem of the plant because of the cytotoxic effects of the fungal growth media against HeLa cancer cells (See *Methods*, section 2.7)

2.2 Identification of Fungus

Endophyte sample 6/35 was assigned to the Xylaria genus through PCR amplification of its ribosomal DNA. A BLAST search showed most of the DNA to have 99% sequence homolgy to Xylaria sp. F14,[2] previously identified as an endophyte obtained from a *Bazzania* plant species in the Blue Mountains of Jamaica. The 18S rDNA sequence of fungus 6/35, however, contains a large insert of 368 bases that matches most closely with part of the 18S sequence of *Rosellinia necatrix* with a score of 139 bits and an E value of 2e-31. This combination of rDNA and insert is not found in the BLAST database. Fungus 6/35 is likely a new species; however, ITS sequence data is needed for further analysis (see *Methods*, section 2.7; and rDNA sequence, section 4.4).

2.3 Compound Isolation

2.3.1 Solvent Extraction

The black and white fungus 6/35 was grown on 1L of M1D media in a 2L flask at 22°C under static conditions for six months. The mycelium was blended in a blender with ethyl acetate, while the 1L of culture filtrate was extracted three times using ethyl acetate. Product from both extractions was combined because of the similarity in their HPLC profiles (Figures 2-1 and 2-2). The solvent was dried down and the yellow product (~1g) was fractionated using ethanol. White precipitate (~200mg) and a yellow oil (~100mg) formed upon addition of ethanol. Cytotoxicity testing was performed on the solid, the oil, and the ethanol-soluble portion.

2.3.2 HPLC

The white solid and the remaining ethanol-soluble portion were analyzed using HPLC (Figure 2-3) using a solvent system of 46% acetonitrile and 54% water with isocratic elution. The yellow oil did not show significant cytotoxic activity, but its HPLC profile is included here (Figure 2-4).

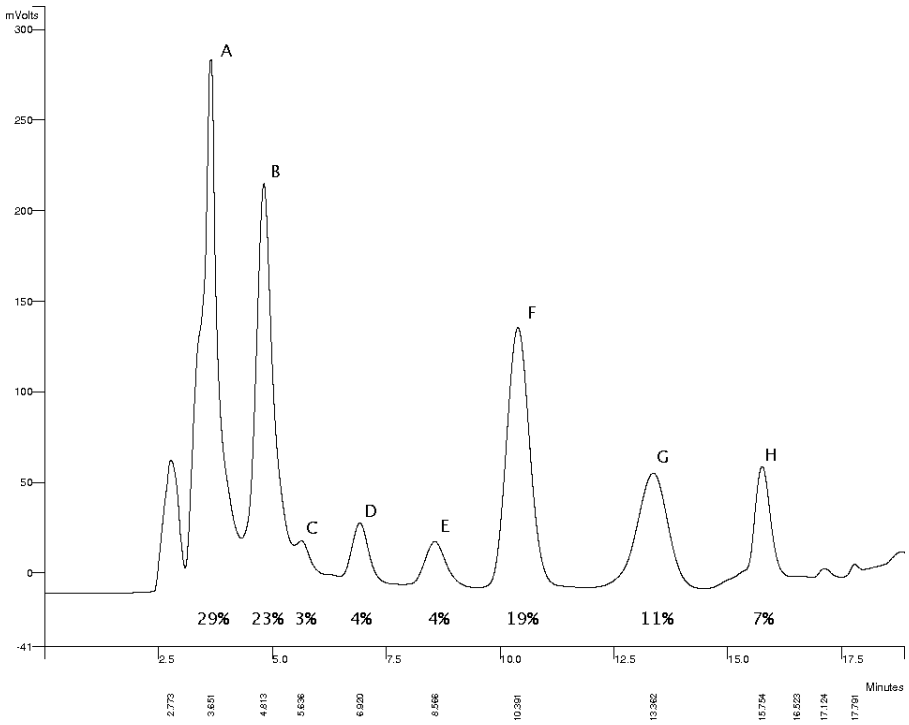

Figure 2-1 HPLC profile of ethyl acetate extraction of endophyte mycelia 6/35; percentage of total peak area is given under each peak.

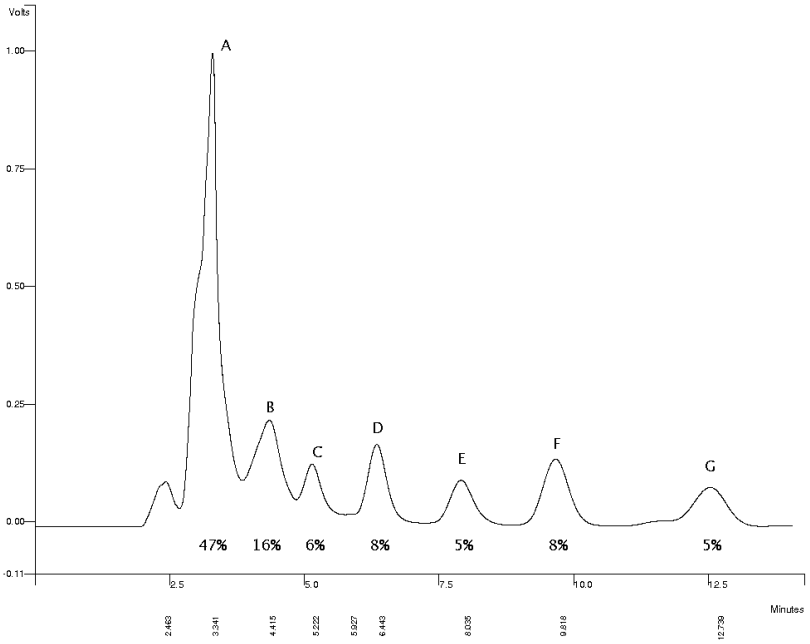

Figure 2-2 HPLC profile of ethyl acetate extraction of growth media of endophyte 6/35; percentage of total peak area is given under each peak.

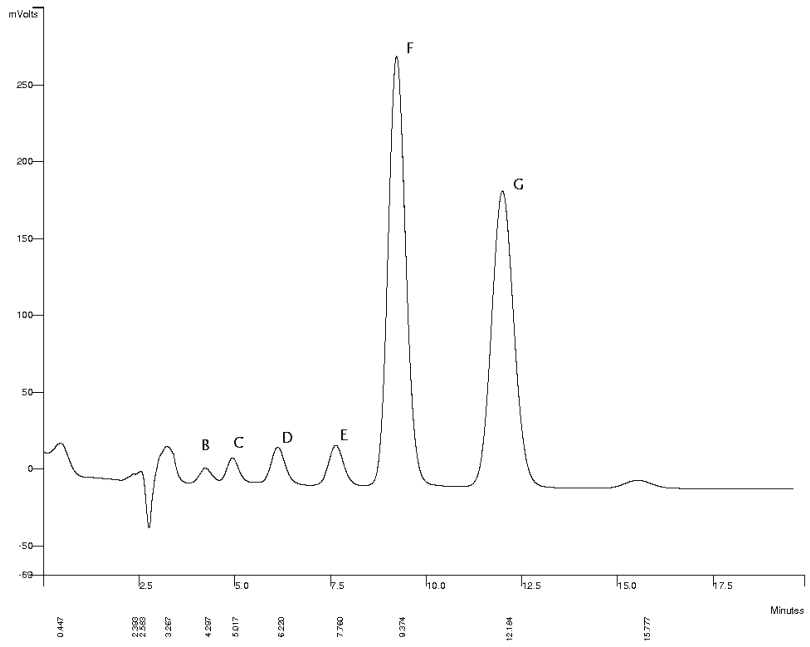

Figure 2-3 HPLC profile of white solid from ethyl acetate extraction of endophyte 6/35 mycelia and growth media.

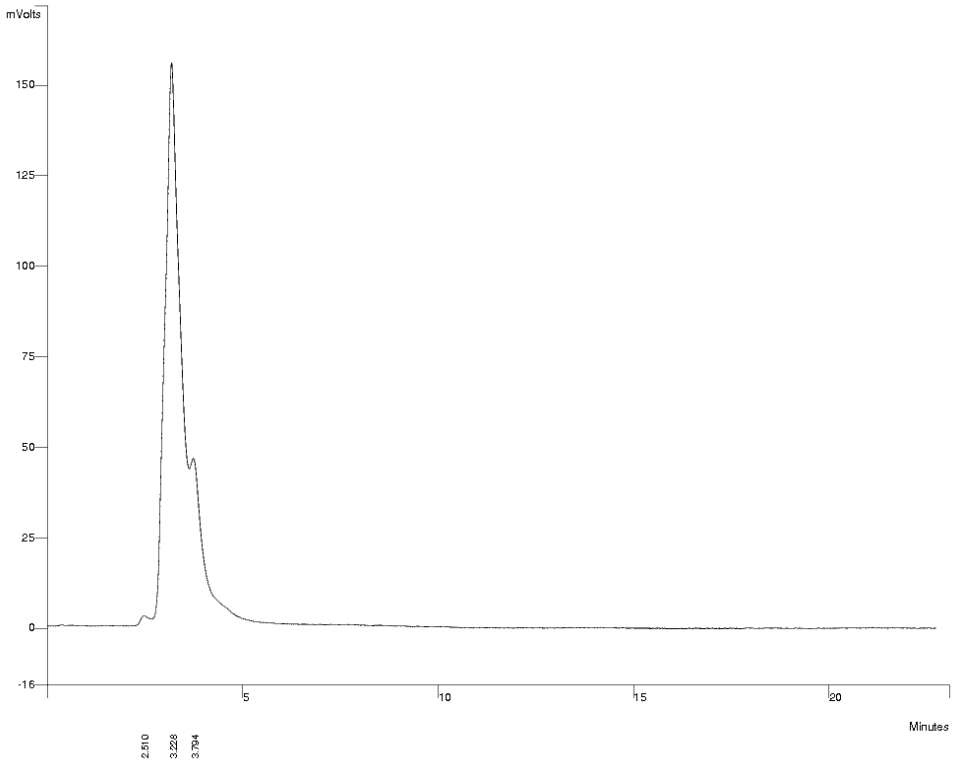

Figure 2-4 HPLC profile of oil produced upon addition of ethanol to dried-down ethyl acetate extraction of endophyte 6/35 mycelia and growth media.

Preparative HPLC was performed on the combined liquid and fungal extract, using a solvent system of 46% acetonitrile and 54% water with isocratic elution. Compounds from peaks D and F were isolated in sufficient purity and quantity to allow for structural determination based on NMR, MS, x-ray crystallography, and IR.

In February of 2005, approximately four months after the original experiment, mycelium grown on M1D media for one month under static conditions at 22°C was extracted using ethyl acetate in the same manner performed previously. Approximately 500 mg of material was isolated. The HPLC profile for this extract (Figure 2-5) was significantly less

complex than the profile for the previous extraction, possibly because of the difference in length of time they were allowed to ferment.

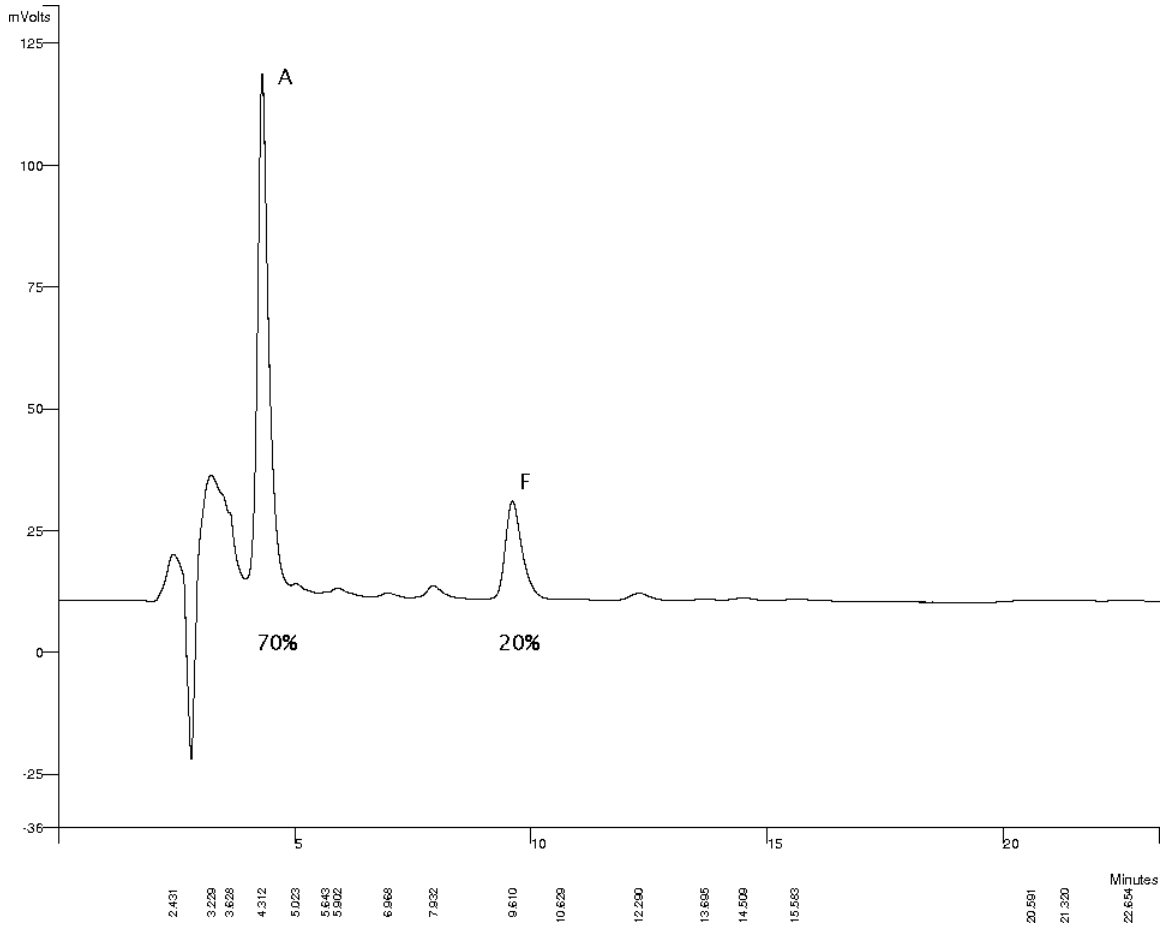

Figure 2-5 HPLC profile of second ethyl acetate extraction of mycelia from endophyte 6/35.

In this second extraction, the HPLC profile did not show a contaminating shoulder peak on the leading edge of peak A, as can be seen on peak A from the first extraction. Peak A was isolated from the second extraction using preparative HPLC (see *methods*, section 2.7) and the structure was determined using NMR, MS, and IR.

2.3.3 Relative Yields

The HPLC profiles were analyzed and the relative yields of each product were roughly estimated based on peak area. The peaks were labeled A through H according to elution order.

The amount of product obtained from peak D after combination of extracts and passage through preparative HPLC was 15 mg. Estimations of the amount of each substance can be obtained by comparison of area percentage on the HPLC profile.

2.4 Activity of the fractions

The fractions obtained after preparative HPLC separation were dried down and tested individually against HeLa cervical cancer cells to determine which fractions were most worthy of pursuit. Thirteen fractions were obtained, and they, along with the white solid and yellow oil, were tested. The results of the assay can be seen in Figure 2-6 and Figure 2-7. The most cytotoxic fractions were analyzed by HPLC to determine which components they contained. Fraction 3 contained mostly material from peak A; fraction 4, peaks A and B; fraction 5, A, B, C, and D; fractions 6 and 7 had peak D; fraction 11 had peak F, and fraction 12 had peaks F, G, and H. All peaks showed at least some HeLa cell growth inhibition.

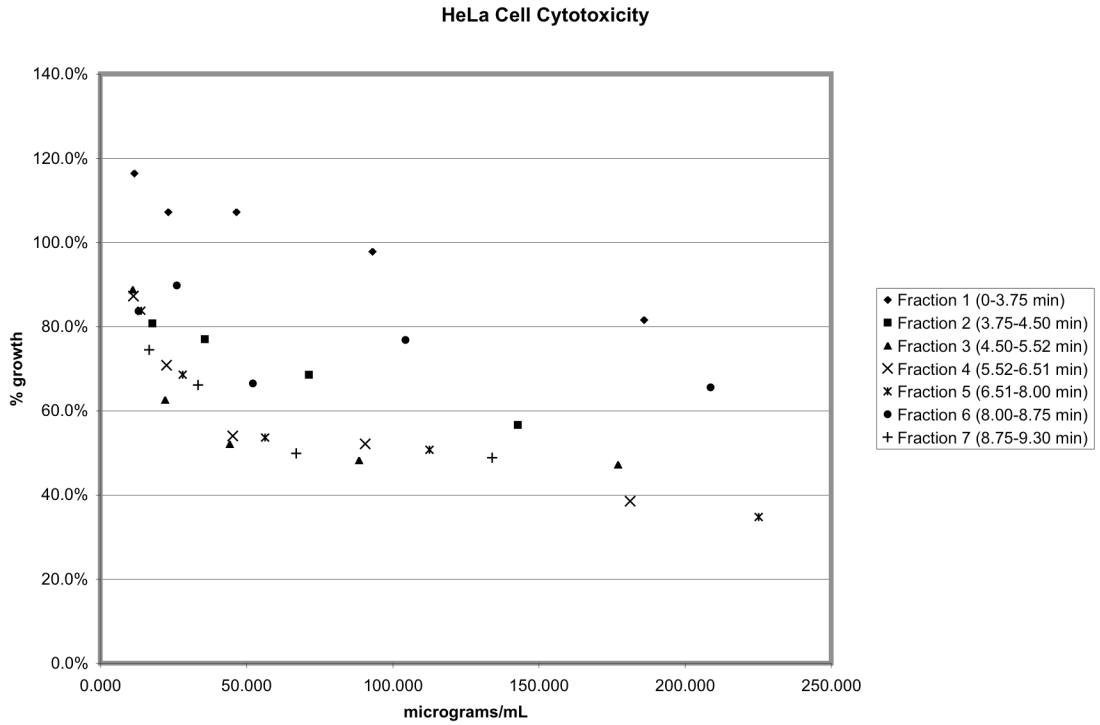

Figure 2-6 Cytotoxicity data for preparative HPLC fractions 1 through 7, obtained at 46% acetonitrile isocratic gradient with flow rate of 20 mL/min.

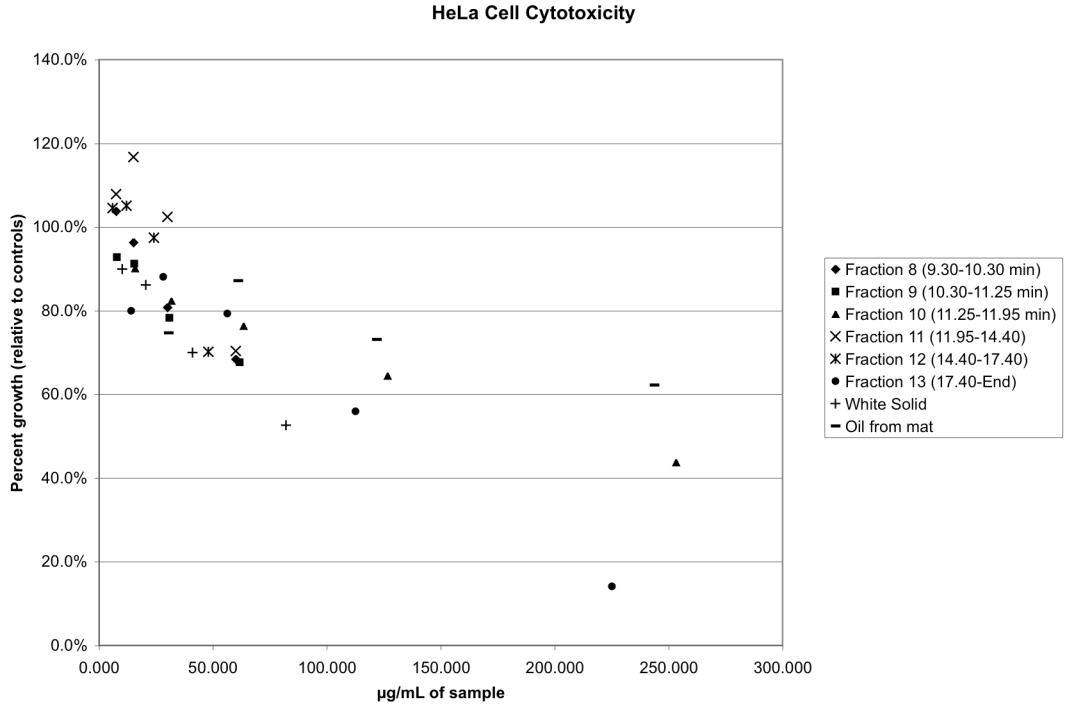

Figure 2-7 Cytotoxicity data for HPLC fractions 8 through 13, the oil, and the white solid, obtained at 46% acetonitrile isocratic gradient with flow rate of 20 mL/min.

2.5 Determination of Structure

2.5.1 Structural Determination of 19,20-Epoxycytochalasin C (Peak F)

Data from several sources were used to identify the compound associated with Peak F after isolation from preparative HPLC. The sodiated m/z from a thioglycerol matrix was 546.2405—the odd mass value after sodium subtraction indicating the presence of nitrogen. The infrared data gave a strong carbonyl peak at 1681 cm^{-1} indicating an amide, a medium carbonyl peak at 1747 cm^{-1} indicating an ester functionality, and methyl and methylene peaks at 2928 cm^{-1} and 2856 cm^{-1}. There was also a broad peak at 3345 cm^{-1}, indicating the presence of -OH groups (see Figure 2-8).

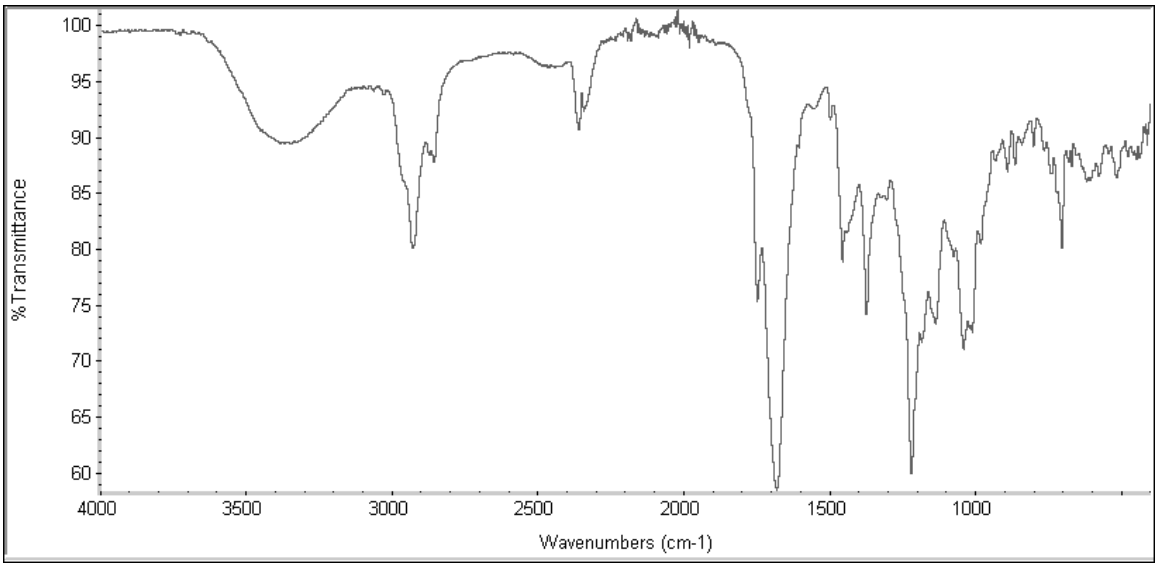

Figure 2-8 Infrared spectrum of Peak F.

NMR experiments were performed in deuterated acetone. Data from ^{1}H NMR, COSY, quantitative ^{13}C, DEPT, and HETCOR were obtained (see *Glossary of NMR terms,*

section 3.2). The protons around δ_H 7 quickly indicated the presence of a phenyl group, while the shifts at δ_H 5.76 and 6.02 indicated a probable alkene group surrounded by protonated carbons, based on their splitting. One peak between these two, which did not exhibit any splitting, was found at δ_H 5.76. This peak was later recognized as C-21 based on comparison with the literature.[3] There were several peaks indicating saturated carbons at δ_H 1.03, 1.15, 1.47, and 1.59. The shifts at δ_H 2.08, 2.17, 2.24, and possibly δ_H 2.52 and 2.53 indicated allylic protons, while several shifts (δ_H 3.06, 3.14, 3.36, 3.39, 3.45, 3.48, and 3.76) were indicative of protons on carbons near oxygen or nitrogen (See Figure 2-9 and Table 2-1).

The quantitative ^{13}C NMR spectrum (Figure 2-11 and Table 2-2) showed the presence of three carbonyl groups at δ_C 171, 175, and 217, and seven benzene and vinylic carbons between δ_C 115 and 140. The data from DEPT (Figure 2-13) and COSY identified which carbons were on the benzene ring. Data from DEPT also assigned proton numbers to the 17 carbons located below δ_C 80ppm. The five lowest shifted carbons had three protons, while two of the carbons were quaternary sp^3 carbons. The rest of the carbons below δ_C 80 were mono-protonated, with the exception of C-15 at δ_C 38.85 (adjacent to the alkene group), and C-10 at δ_C 45.04 (the carbon connected to the benzene ring). Two suspect peaks in the ^{13}C spectrum at δ_C 23.4 and 32.7 were found to be from contamination and were ignored.

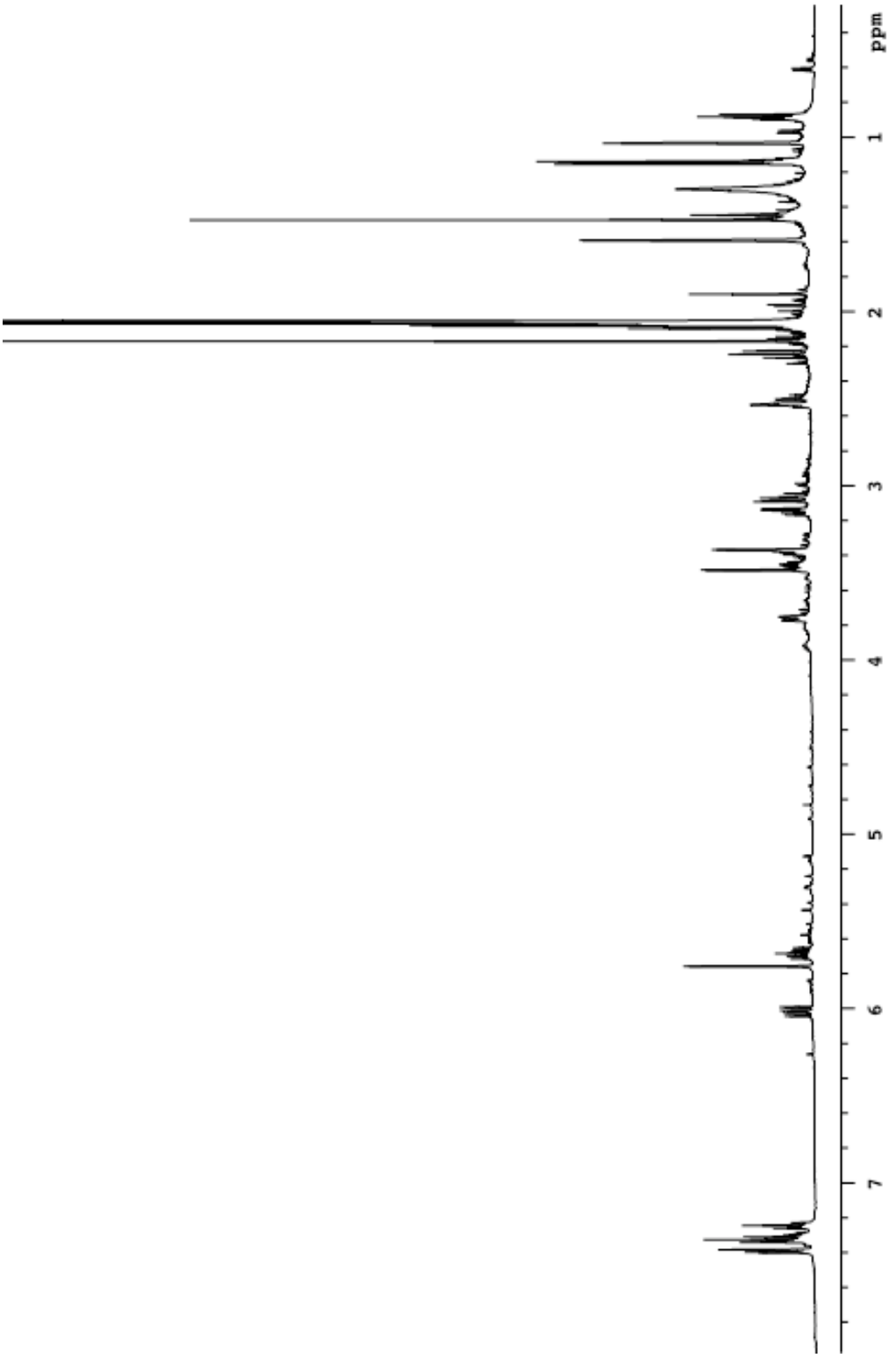

Figure 2-9 500 MHz ^{1}H NMR of Peak F in acetone.

Table 2-1 ^{1}H NMR Shift values for 19, 20-epoxycytochalasin C and the compound isolated from Peak F

19, 20-epoxycytochalasin C*			Peak F		
Carbon	Shift	Splitting	Carbon	Shift	Splitting
NH	5.56	br s			
3	3.33	dd (8.2,6.7)	3	3.39	m
4	2.52	br s	4	2.53	br s
5			5		
7	3.78	br d (9.8)	7	3.76	d
8	2.26	dd (10.2,9.8)	8	2.24	dd
10	3.06	dd (13.5,6.0)	10	3.06	dd
10	2.99	dd (13.5,9.2)	10	3.14	dd
11	1.41	s	11	1.59	s
12	1.65	s	12	1.03	s
12			12		
13	6.13	dd (15.7,10.2)	13	6.02	dd
14	5.7	ddd (15.8,9.9,6.1)	14	5.68	dddd
15	2.67	ddd (12.6,10.1,10.0)	15	2.08	?
15	2.09	m	15	2.52	dd
16	3.22	ddq (10.8,6.7,1.2)	16	3.45	ddd
19	3.19	d (2.0)	19	3.48	d
20	3.43	dd (2.0,0.8)	20	3.36	m
21	5.74	br s	21	5.76	s
22	1.18	d (6.7)	22	1.15	d
23	1.5	s	23	1.47	s
25	2.14	s	25	2.17	s
2',6'	7.31	m	2',6'	7.39	d
3',5'	7.19	m	3',5'	7.31	t
4'	7.25	m	4'	7.24	t

*Data from Espada, A.; Rivera-Sagredo, A.; de la Fuente, J.M.; Hueso-Rodriguez, J. A.: Elson, S. W. Tetrahedron 1997, 53, 6485-6492.

The COSY correlation of ^{1}H NMR shifts proved useful in identifying the connectivities of those protons on the more saturated side of the compound (Figure 2-10). The 2D spectra showed the connectivity of the protons associated with C-7, C-8, C-13, C-14, C-15, C-16, and C-22. It also showed the connection between protons on C-19, C-20, and C-21. The HETCOR 3D spectrum was needed to determine the correlation of proton shifts with the carbon shifts. The correlation data is shown graphically (Figure 2-13). Each proton peak from the compound showed corrct correlation with its carbon.

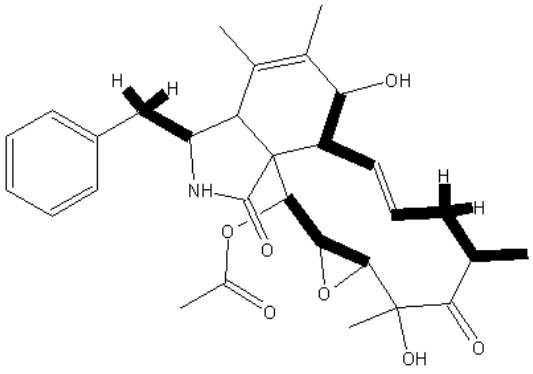


```
COSY of Sample-11

Pulse Sequence: relayh

 Solvent: Acetone
 Ambient temperature
File: COSY
INOVA-500  "nmr500"

 Relax. delay 0.400 sec
 COSY 90-90
 Acq. time 0.128 sec
 Width     8000.0 Hz
 2D Width 8000.0 Hz
 4 repetitions
 512 increments
OBSERVE   H1, 499.9159684 MHz
DATA PROCESSING
 Sine bell 0.064 sec
F1 DATA PROCESSING
 Sine bell 0.032 sec
FT size 2048 x 2048
Total time 19 min, 29 sec
```

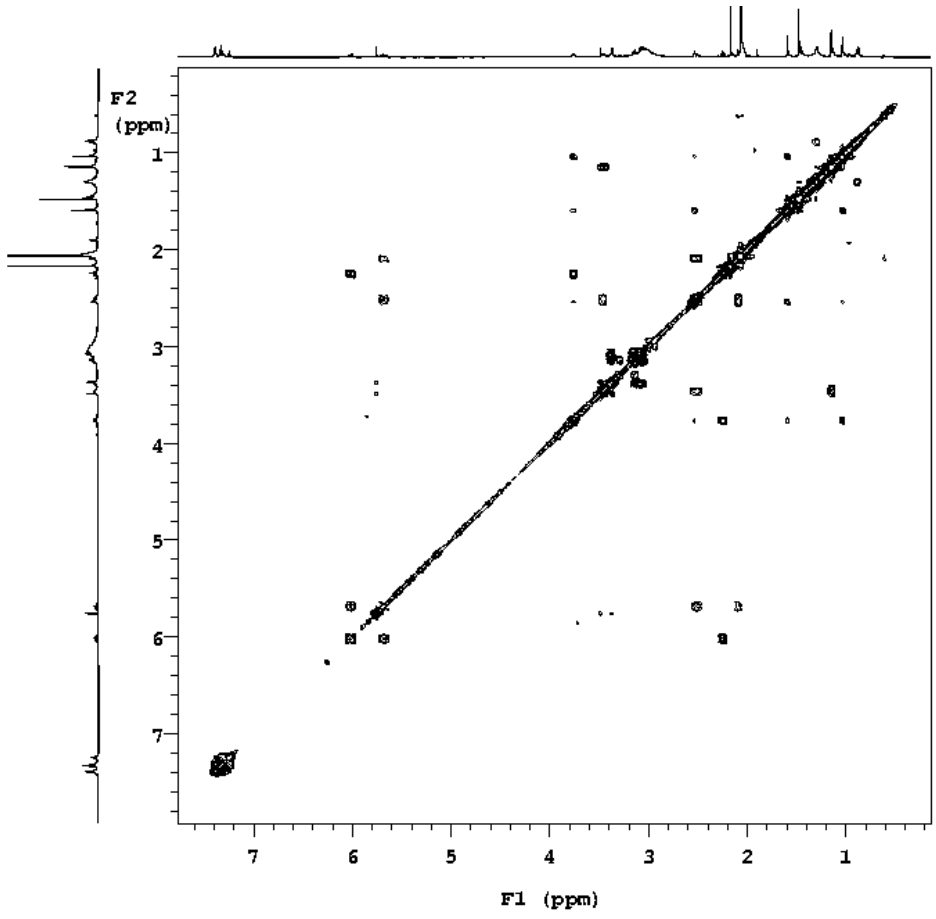

Figure 2-10 ^{1}H-^{1}H COSY spectrum of 19,20 epoxycytochalasin C (Peak F); connectivities shown in bold.

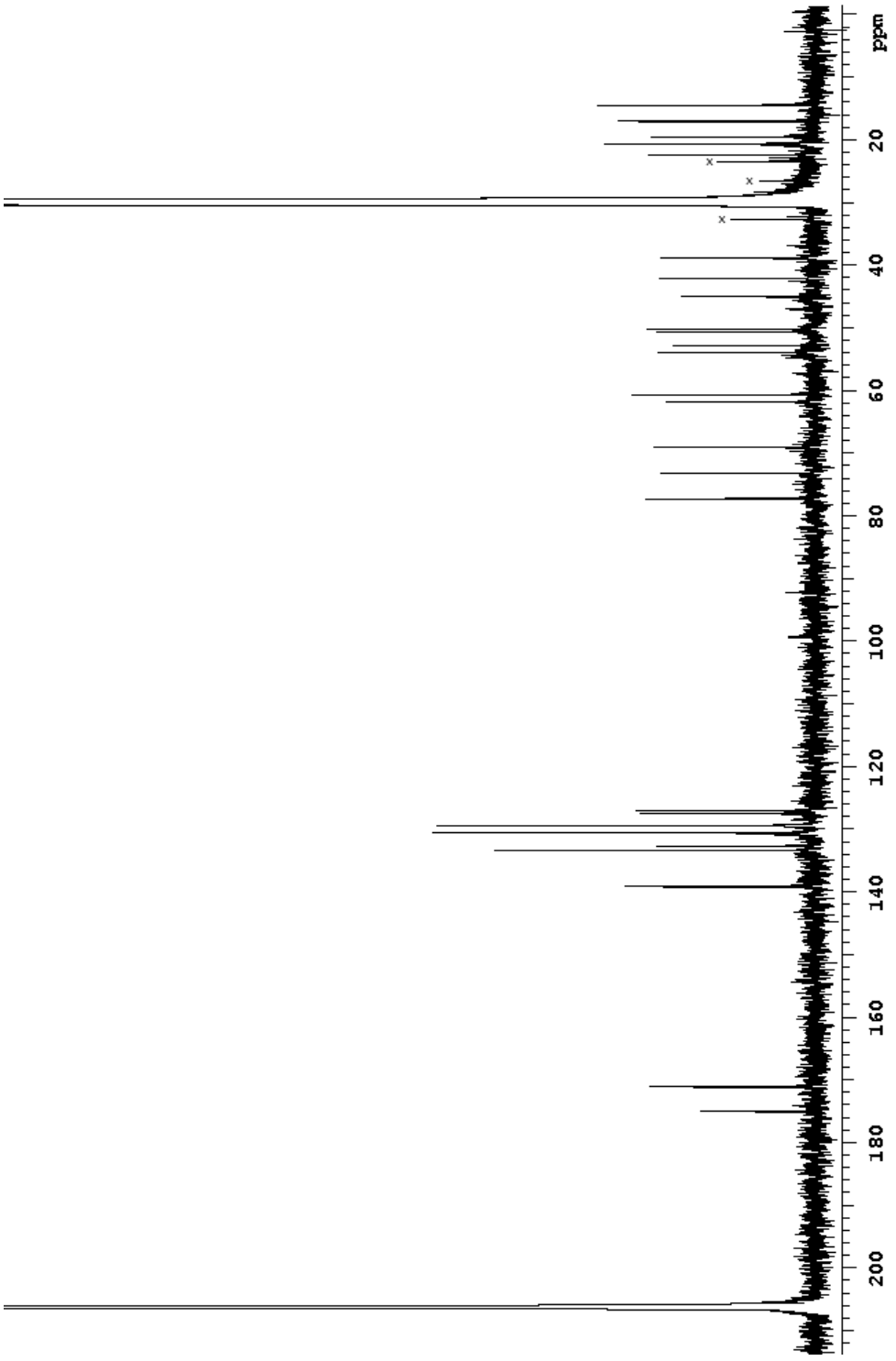

Figure 2-11 500 MHz quantitative ^{13}C NMR spectrum of Peak F in acetone; x indicates contamination peak.

Table 2-2 ^{13}C NMR shift values of 19,20-epoxycytochalasin C in $CDCl_3$ and Peak F in acetone.

19, 20-epoxycytochalasin C*			Peak F		
Carbon	Shift	Splitting	Carbon	Shift	DEPT
1	174.03	s	1	175.05	s
3	60.62	d	3	61.77	d
4	50.66	d	4	50.63	d
5	126.53	s	5	127.10	s
6	131.29	s	6	132.64	s
7	68.01	d	7	69.04	d
8	49.16	d	8	50.23	d
9	51.39	s	9	52.88	s
10	44.69	t	10	45.04	t
11	13.93	q	11	14.47	q
12	17.12	q	12	17.04	q
13	133.89	d	13	133.38	d
14	131.61	d	14	133.38	d
15	37.36	t	15	38.85	t
16	41.81	d	16	42.10	d
17	215.22	s	17	217.00	s
18	76.29	s	18	77.24	s
19	59.86	d	19	60.64	d
20	53.01	d	20	53.99	d
21	71.93	d	21	73.25	d
22	19.18	q	22	19.51	q
23	21.86	q	23	22.41	q
24	170.05	s	24	171.12	s
25	20.76	q	25	20.74	q
1'	137.46	s	1'	139.16	s
2',6'	129.08	d	2',6'	130.60	d
3',5'	128.92	d	3',5'	129.45	d
4'	127.02	d	4'	127.51	d

*Data from Espada, A.; Rivera-Sagredo, A.; de la Fuente, J.M.; Hueso-Rodriguez, J. A.; Elson, S. W. Tetrahedron 1997, 53, 6485-6492.

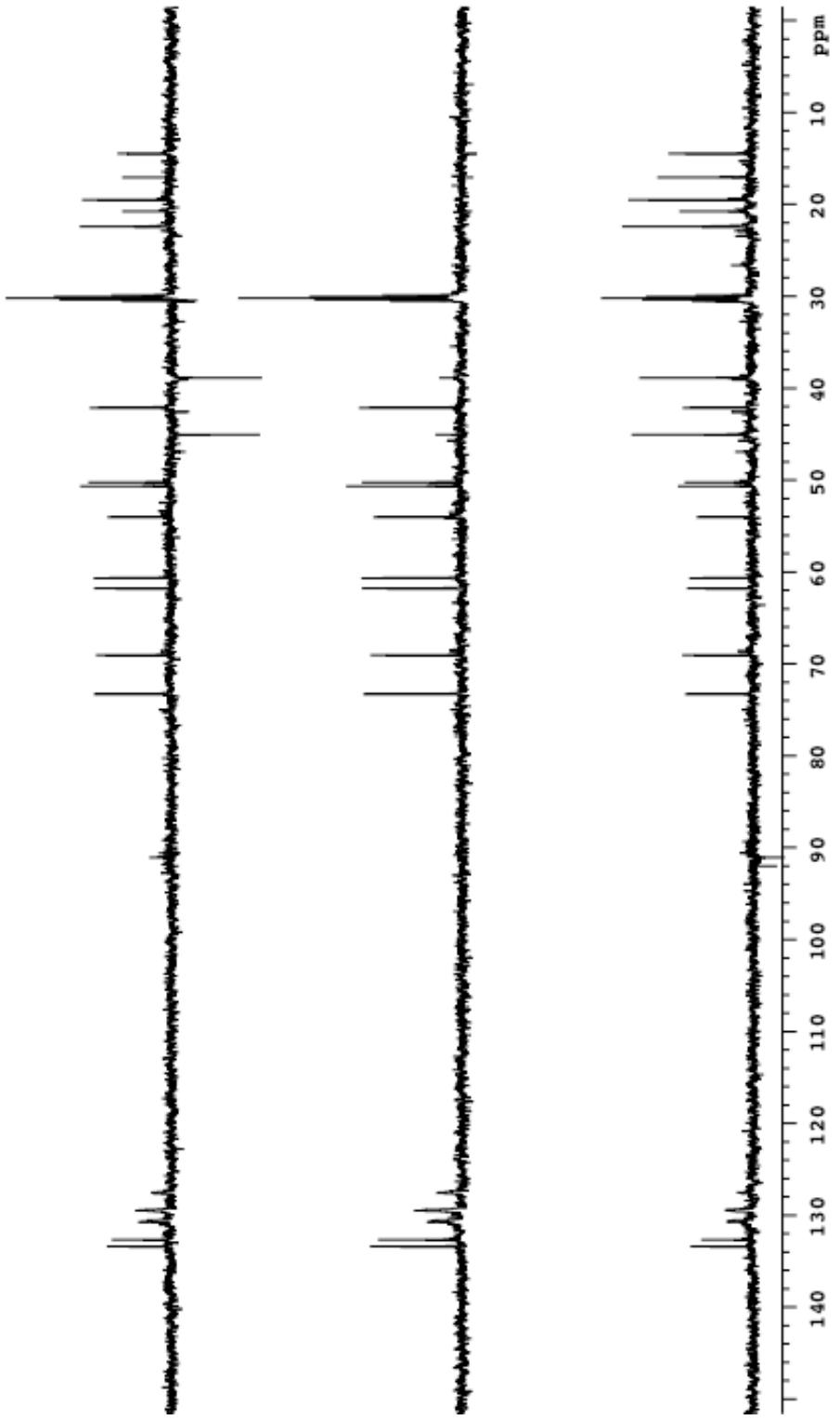

Figure 2-12 DEPT spectrum of Peak F in acetone.

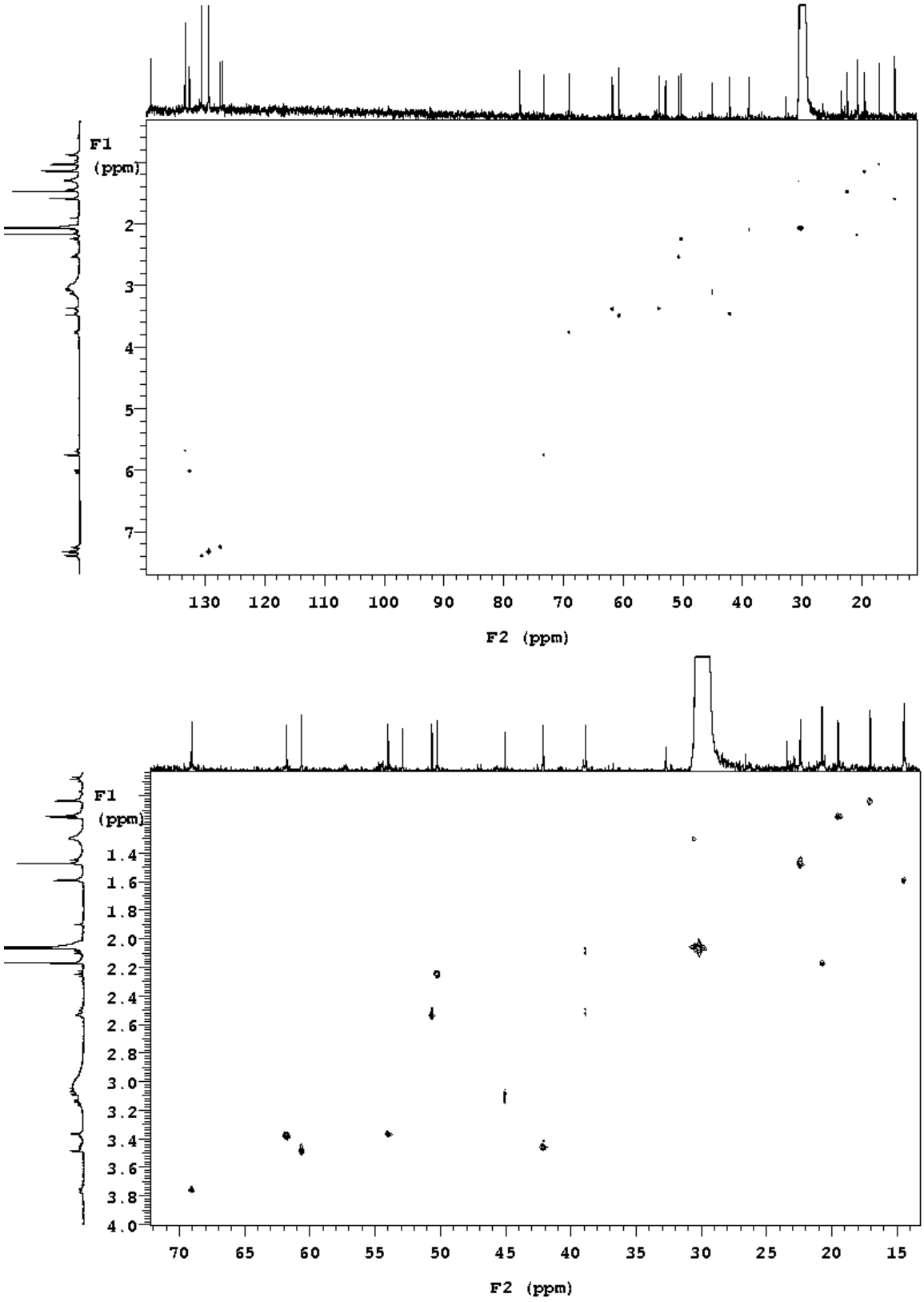

Figure 2-13 HETCOR data for Peak F. **Figure 2-14** Scaled HETCOR data for Peak F.

Small crystals were found in the vial of purified peak F, which were submitted for X-ray analysis. The R-value for the proposed structure was very low (see *Crystal Structure Data for Peak F,* section 3.1). The crystal data was consistent with all other data.

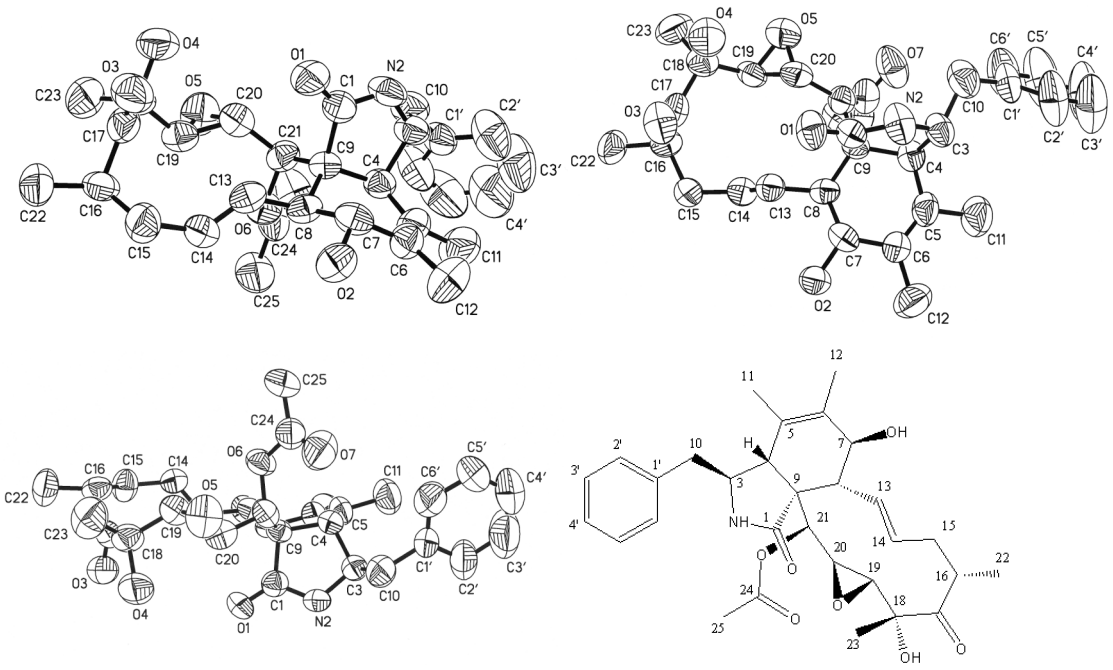

Figure 2-15 Crystal structure ORTEP views of 19,20 epoxycytochalasin C (Peak F).

The NMR spectral data were found to be identical with the values for the known compound 19,20 epoxycytochalasin C, discovered simultaneously by Espada et al and Abate et al [3,4] in 1997. The class of compounds known as cytochalasins will be discussed further in section 2.6.2.

2.5.2 Structural Determination of 19,20-Epoxycytochalasin D (Peak D)

Data were obtained for the compound associated with peak D, and its structure elucidated using NMR, IR and mass spectrometry. DEPT, HMBC and HMQC correlations were performed on this compound (Figures 2-21, 2-17 and 2-22).

The IR data (Figure 2-16) were nearly identical to the data for 19,20-epoxycytochalasin C. The protonated m/z from electrospray ionization mass spectrometry was 524.2603—equal to the apparent mass of 19,20-epoxycytochalasin C. The ^{1}HNMR data (see Figure 2-18 and Table 2-3) were also very similar to the data for Peak F, with the extra singlet peaks at δ_H 5.06 and 5.27 being most salient. These peaks did not correlate with any other proton peaks in the COSY spectrum except with each other; they were therefore designated as peaks from a terminal alkene group linked to a non-protonated carbon. The presence of an extra ^{13}C peak at δ_C 112 bore out this conclusion. Since the ^{1}H spectrum was most different from the spectrum of 19,20-epoxycytochalasin C at the protons associated with C-3 through C-6 and their substituents, and since the apparent mass of the two compounds was identical,

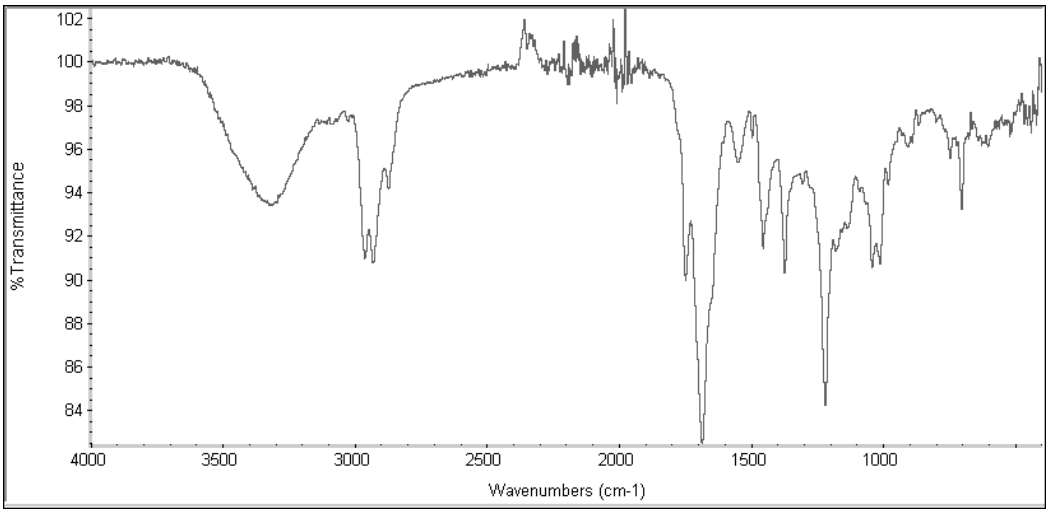

Figure 2-16 Infrared Spectrum of Peak D.

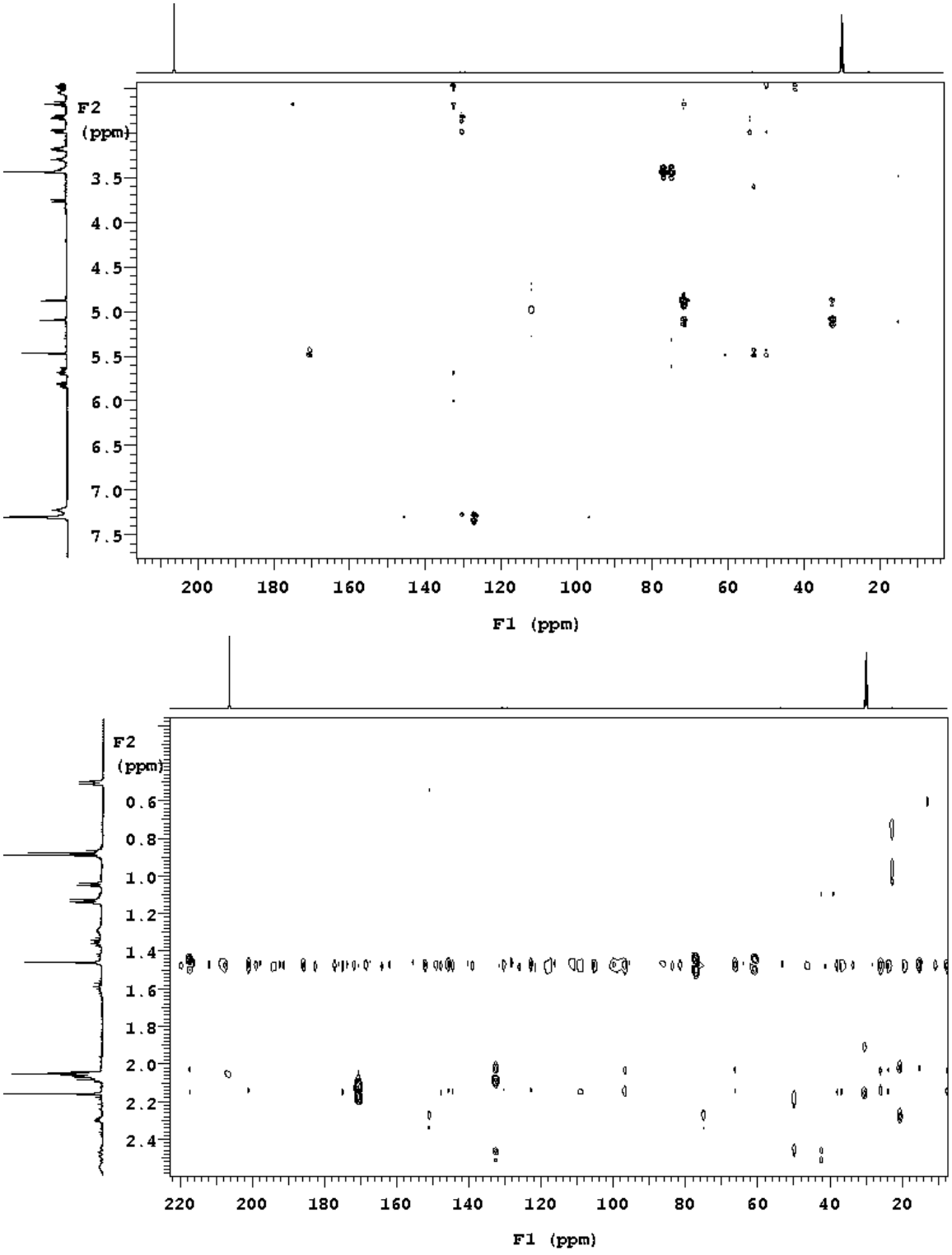

Figure 2-17 HMBC of Peak D in acetone.

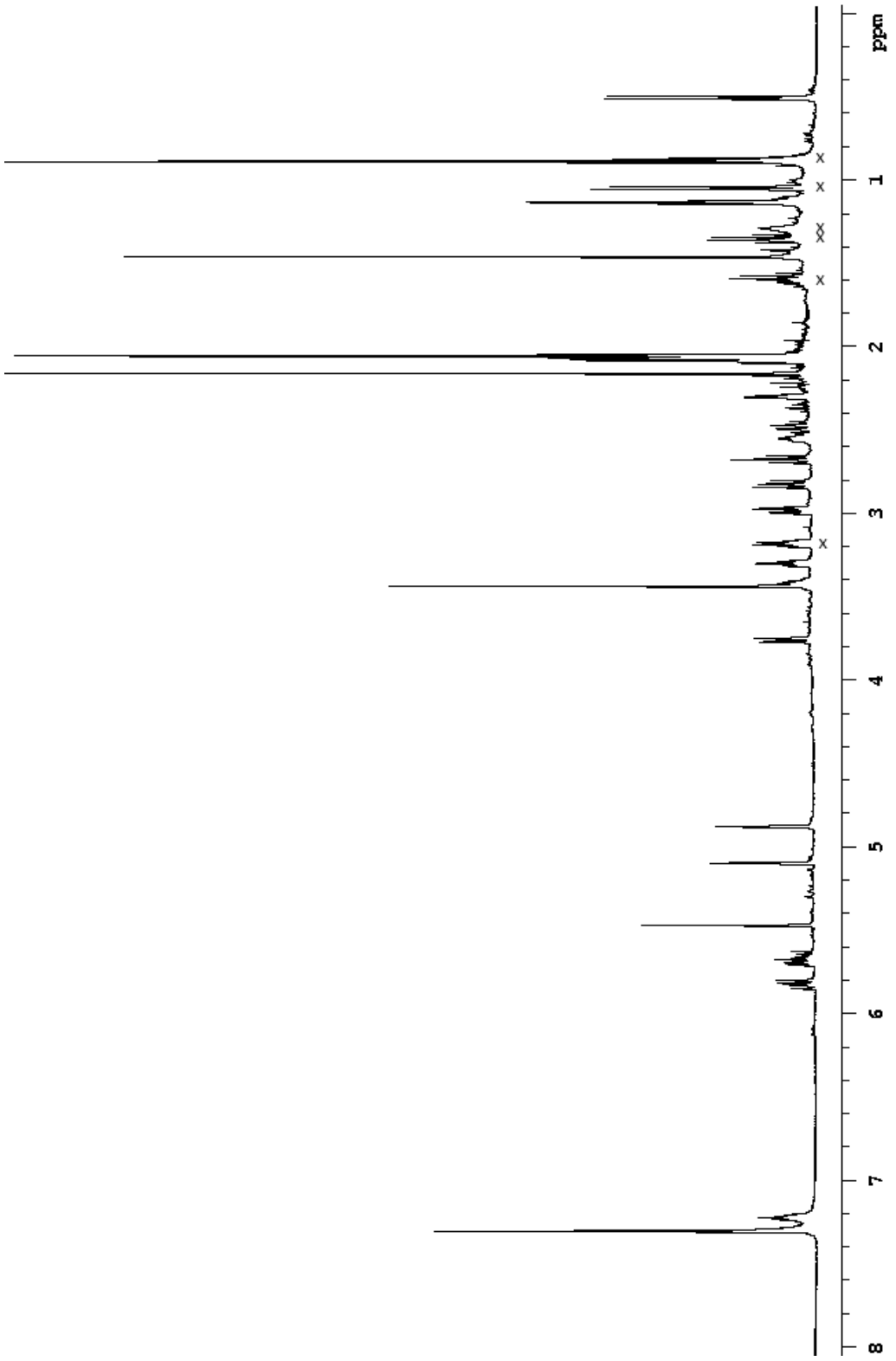

Figure 2-18 500 MHz ^{1}H NMR spectrum of Peak D in acetone; (x) indicates extraneous peaks.

Table 2-3 ^{1}H NMR data of Peak D in acetone.

19, 20-epoxycytochalasin D*			Peak D		
Carbon	Shift	Splitting	Carbon	Shift	Splitting
NH	5.46	br s	NH		
3	3.24	M	3	3.31	T
4	2.25	dd (5.2,3.3)	4	2.29	Dd
5	2.62	M	5	2.54	T
7	3.81	br d (10.1)	7	3.78	D
8	2.62	M	8	2.68	T
10	2.85	dd (13.4,5.0)	10	2.81	Dd
10	2.73	dd (13.4,9.1)	10	2.98	Dd
11	0.89	d (6.9)	11	0.88	D
12	5.27	br s	12	5.11	S
12	5.06	br s	12	4.88	S
13	5.89	dd (15.5,9.8)	13	5.81	M
14	5.69	ddd (15.5,9.9,5.8)	14	5.69	M
15	2.62	M	15	2.09	M
15	2.09	M	15	2.48	Dd
16	3.22	M	16	3.41	M
19	3.14	d (1.9)	19	3.42	S
20	3.53	dd (1.9,0.8)	20	3.42	S
21	5.51	br s	21	5.47	S
22	1.18	d (6.6)	22	1.13	D
23	1.53	S	23	1.46	S
25	2.14	S	25	2.15	S
2',6'	7.32	M	2',6'	7.22	M
3',5'	7.15	M	3',5'	7.31	M
4'	7.24	M	4'	7.32	M

*Data from Espada, A.; Rivera-Sagredo, A.; de la Fuente, J.M.; Hueso-Rodriguez, J. A.; Elson, S. W. Tetrahedron 1997, 53, 6485-6492.

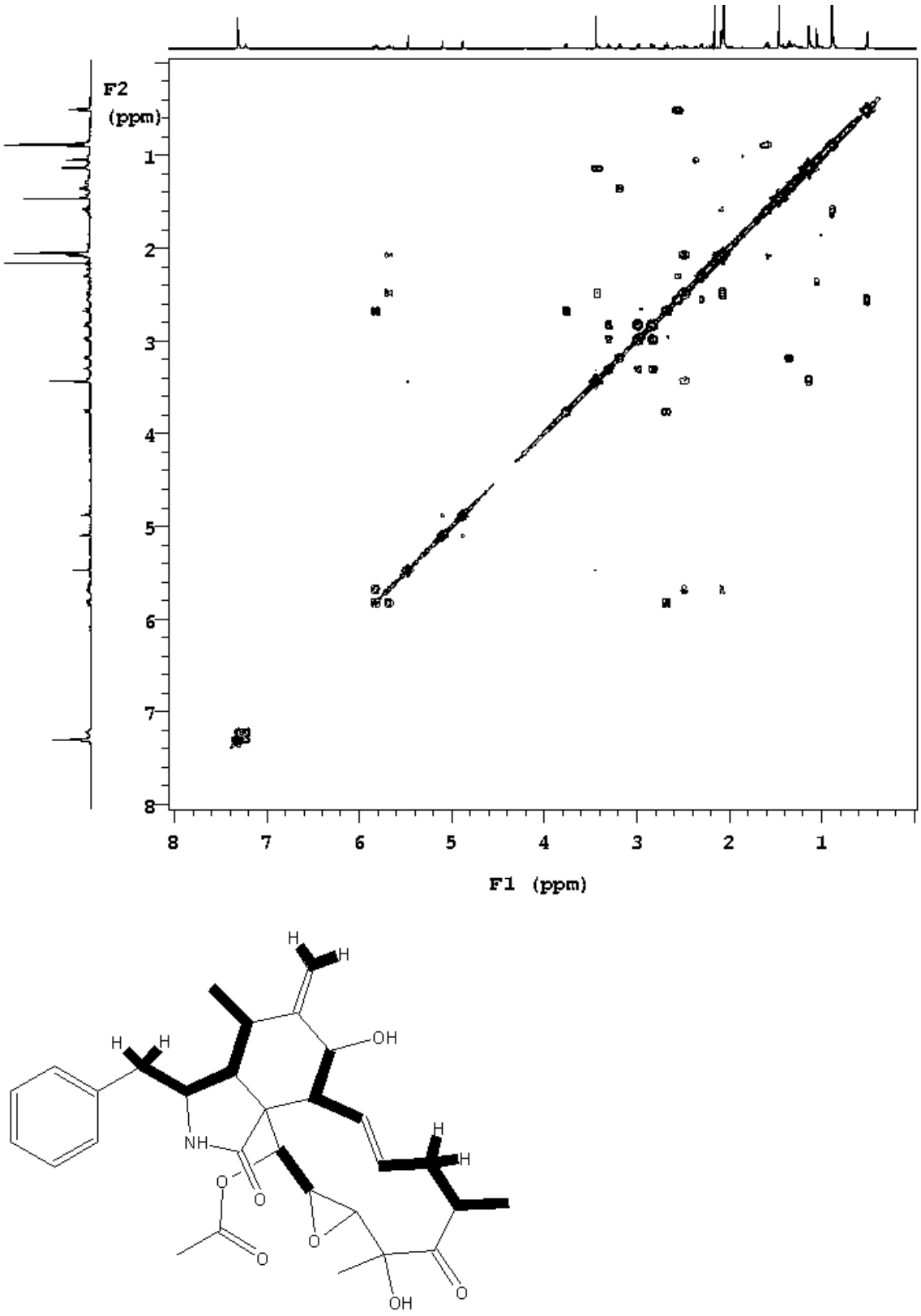

Figure 2-19 ^{1}H-^{1}H COSY spectrum of Peak D.

it was postulated that the location of the double bond between C-5 and C-6 was shifted relative to its position on 19,20-epoxycytochalasin C. The COSY correlation data also established the connectivity of the atoms in this compound as being similar to the connectivity of 19,20 epoxycytochalasin C, with a few important exceptions (Figure 2-19).

The ^{13}C NMR data for this compound (Figure 2-20 and Table 2-4) were surprisingly intermingled with contaminating peaks. Since the HPLC showed only one peak, and since the FAB-MS showed inconclusive results, ESI-MS was performed to determine the nature of the compound and any contaminants. The ESI-MS experiment showed a preponderance of peaks correlating with the monomer, dimer, or trimer of mass 523, with sodium often being the charged species. The only mass that could not be shown to be a breakdown product of the 523 species had a m/z ratio of 232.24 amu. This species associated with the species of mass 523, presenting with a m/z ratio of 755.5 amu and 1278.7 amu. This species could not be identified; however, its presence in the NMR mixture may have contributed to the contamination in the ^{13}C spectrum not only by virtue of its own carbons, but its association with the species of mass 523 in solution may have produced several new ^{13}C shifts in the latter compound by way of an altered electronic environment. This hypothesis is based on the presence in the ^{13}C NMR spectrum of several ^{13}C doublets at real peak locations. There were several contaminating peaks in the ^{1}H NMR spectrum—at δ_H 0.88, 1.29, 1.46, 1.60, and 3.18. The DEPT spectrum and HMQC data are shown in Figure 2-21 and Figure 2-22.

Comparison of the ^{1}H NMR, ^{1}H-^{1}H COSY, and ^{13}C spectrum with the literature showed conclusively that peak D is 19,20-epoxycytochalasin D, which was discovered in *Xylaria hypoxylon* by Espada et al in 1997.[3] A perspective drawing of 19,20-epoxycytochalasin D is shown in Figure 2-23.

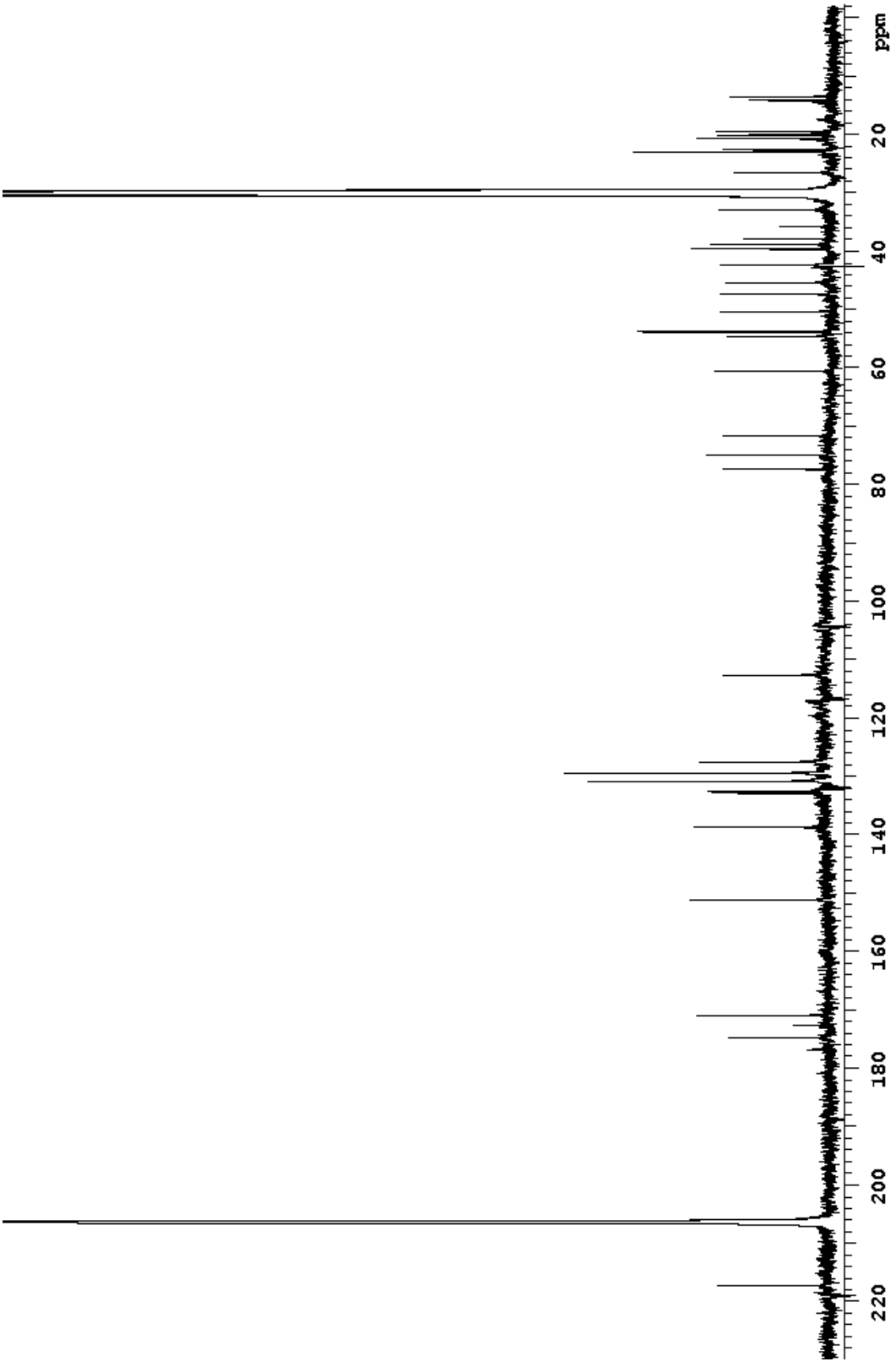

Figure 2-20 500 MHz quantitative ^{13}C NMR of Peak D in acetone.

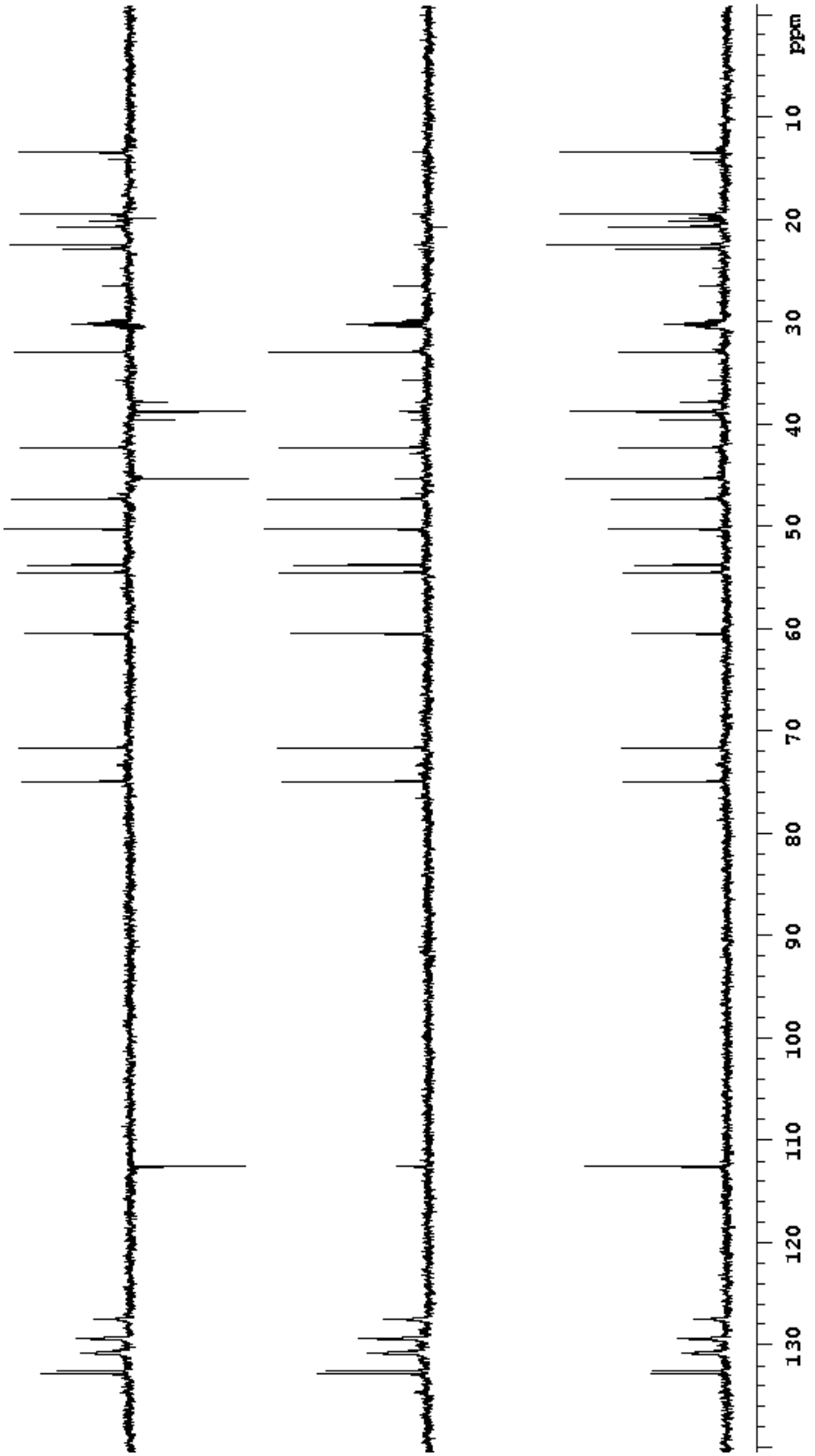

Figure 2-21 DEPT spectrum of Peak D in acetone.

Table 2-4 ^{13}C NMR shift values and DEPT data of Peak D and 19,20-epoxycytochalasin D.

19, 20-epoxycytochalasin D*			Peak D		
Carbon	Shift	DEPT	Carbon	Shift	DEPT
1	173.43	s	1	174.74	s
3	53.90	d	3	54.48	d
4	50.71	d	4	50.25	d
5	32.56	d	5	32.92	d
6	147.35	s	6	151.04	s
7	69.98	d	7	71.62	d
8	46.54	d	8	47.29	d
9	52.45	s	9	52.67	s
10	45.18	t	10	45.28	t
11	13.49	q	11	13.41	q
12	114.44	t	12	112.52	t
13	131.17	d	13	132.44	d
14	133.47	d	14	132.76	d
15	37.40	t	15	37.80	t
16	41.89	d	16	42.26	d
17	215.28	s	17	217.22	s
18	76.32	s	18	77.32	s
19	59.63	d	19	60.46	d
20	52.72	d	20	53.73	d
21	74.06	d	21	74.90	d
22	19.17	q	22	19.50	q
23	21.86	q	23	22.45	q
24	169.82	s	24	170.81	s
25	20.68	q	25	20.65	q
1'	137.11	s	1'	138.66	s
2',6'	129.14	d	2',6'	129.32	d
3',5'	128.97	d	3',5'	130.75	d
4'	127.13	d	4'	127.42	d

*Data from Espada, A.; Rivera-Sagredo, A.; de la Fuente, J.M.; Hueso-Rodriguez, J. A.; Elson, S. W. Tetrahedron 1997, 53, 6485-6492.

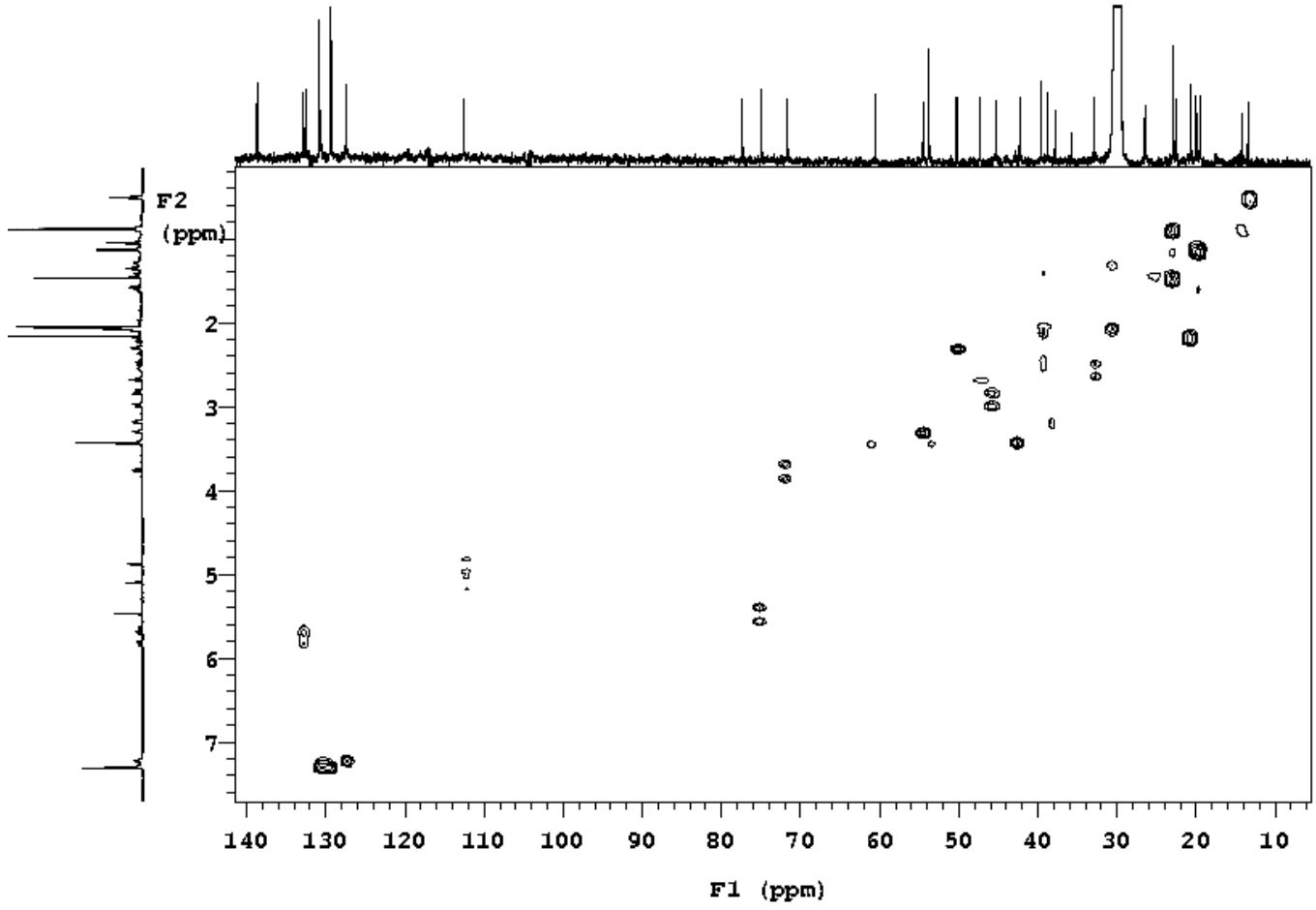

Figure 2-22 HMQC correlation data for Peak D.

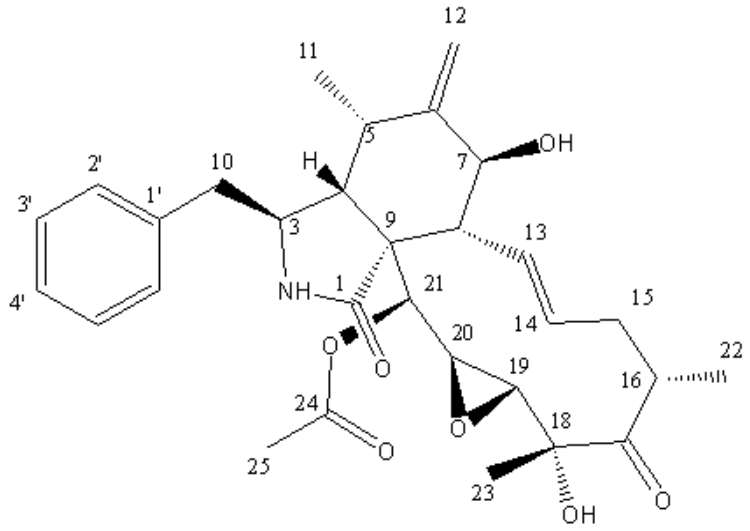

Figure 2-23 19,20-epoxycytochalasin D.

2.5.3 Structural Determination of Xylobovide

Peak A from the second mat extraction was isolated using preparative HPLC and analyzed using IR, FAB-MS, ^{1}H NMR, ^{1}H-^{1}H COSY, HMBC, HMQC, and ^{13}C NMR spectroscopy.

The IR peak at 1769 cm^{-1} in conjunction with NMR data suggested a lactone ring structure, and peaks near 2976 cm^{-1} showed the presence of methyl and methylene groups (see Figure 2-24).

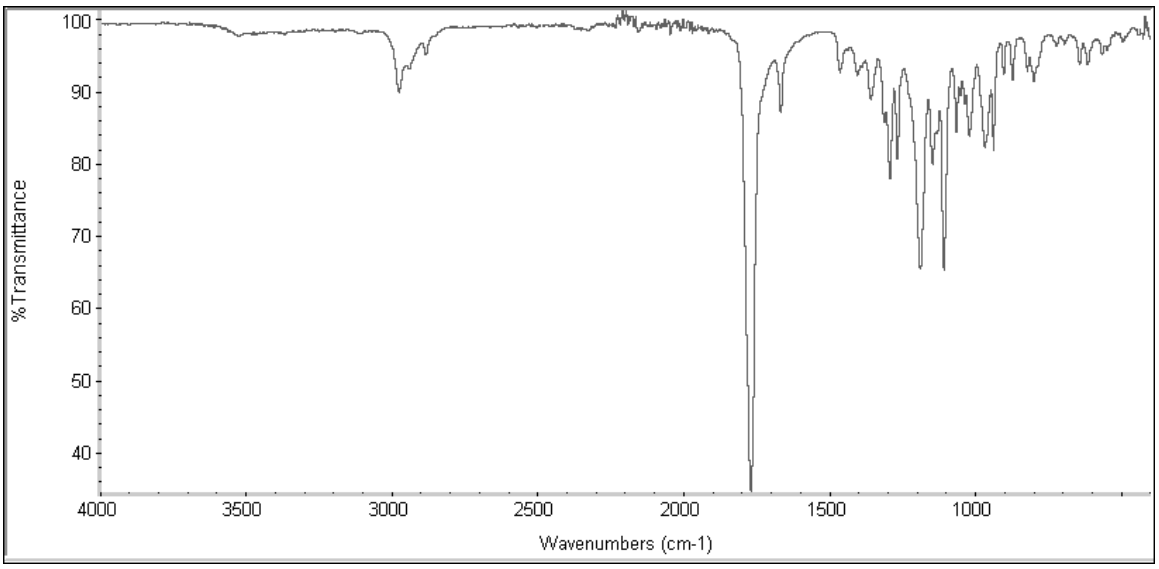

Figure 2-24 IR spectrum of Peak A.

The ^{1}H NMR and COSY spectra in $CDCl_3$ showed the presence of an ethyl group with peaks at δ_H 1.12 (t, J = 7.5 Hz) and 1.94 (qd, J = 7, 7.5 Hz), two methines consistent with lactone ring structure at δ_H 4.6 (td, J = 7.5, 4.75 Hz) and 5.18 (dd, J = 7, 4.75 Hz), and another methine at δ_H 4.03 (td, J = 2, 7 Hz). Two peaks, at δ_H 6.17 (d, J = 2 Hz) and 6.48 (d, J = 2 Hz), suggested terminal alkene functionality (Figure 2-25 and Table 2-5).

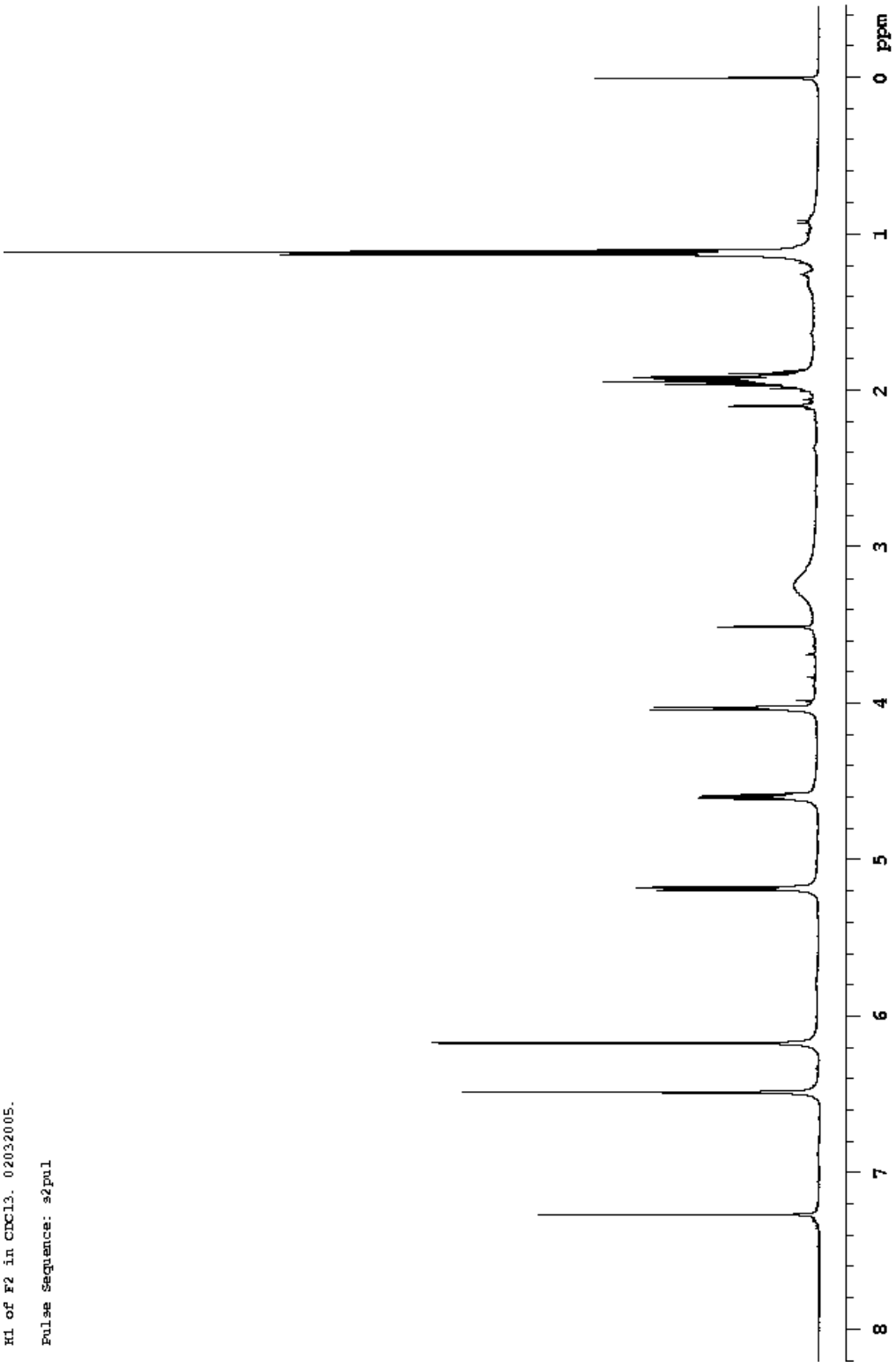

Figure 2-25 500 MHz ^{1}H NMR spectrum of Peak A in $CDCl_3$

Table 2-5 ^{1}H NMR shift values for Peak A in $CDCl_3$

Xylobovide*			Peak A		
Carbon	Shift	Splitting	Carbon	Shift	Splitting
1	1.05	t (7.5)	1	1.12	t (7.5)
2	1.85	qtd (7.5, 7.5, 4.5)	2	1.94	qd (7, 7.5)
3	4.55	td (7.5, 4.5)	3	4.6	td (7.5, 4.75)
4	5.14	dd (7, 4.5)	4	5.18	dd (7, 4.75)
5	not incl.		5	4.03	td (2, 7)
8	6.4	d (2)	8	6.48	d (2)
8'	6.1	d (2)	8'	6.17	d (2)
*Data taken from Abate, D.; Abraham, W. R.; Meyer, H. Phytochemistry 1997, 44, 1443-1448.					

Table 2-6 ^{13}C NMR shift values of Peak A in $CDCl_3$

Xylobovide*			Peak A	
Carbon	Shift	DEPT	Carbon	Shift
1	9.7	q	1	9.8
2	22.1	t	2	22.2
3	77.1	d	3	84
4	84.3	d	4	77.2
5	46.3	d	5	46.2
6	129.9	s	6	129.7
7	167.7	s	7	167.4
8	127.3	t	8	127.4
9	172.4	s	9	172.1
*Data taken from Abate, D.; Abraham, W. R.; Meyer, H. Phytochemistry 1997, 44, 1443-1448.				

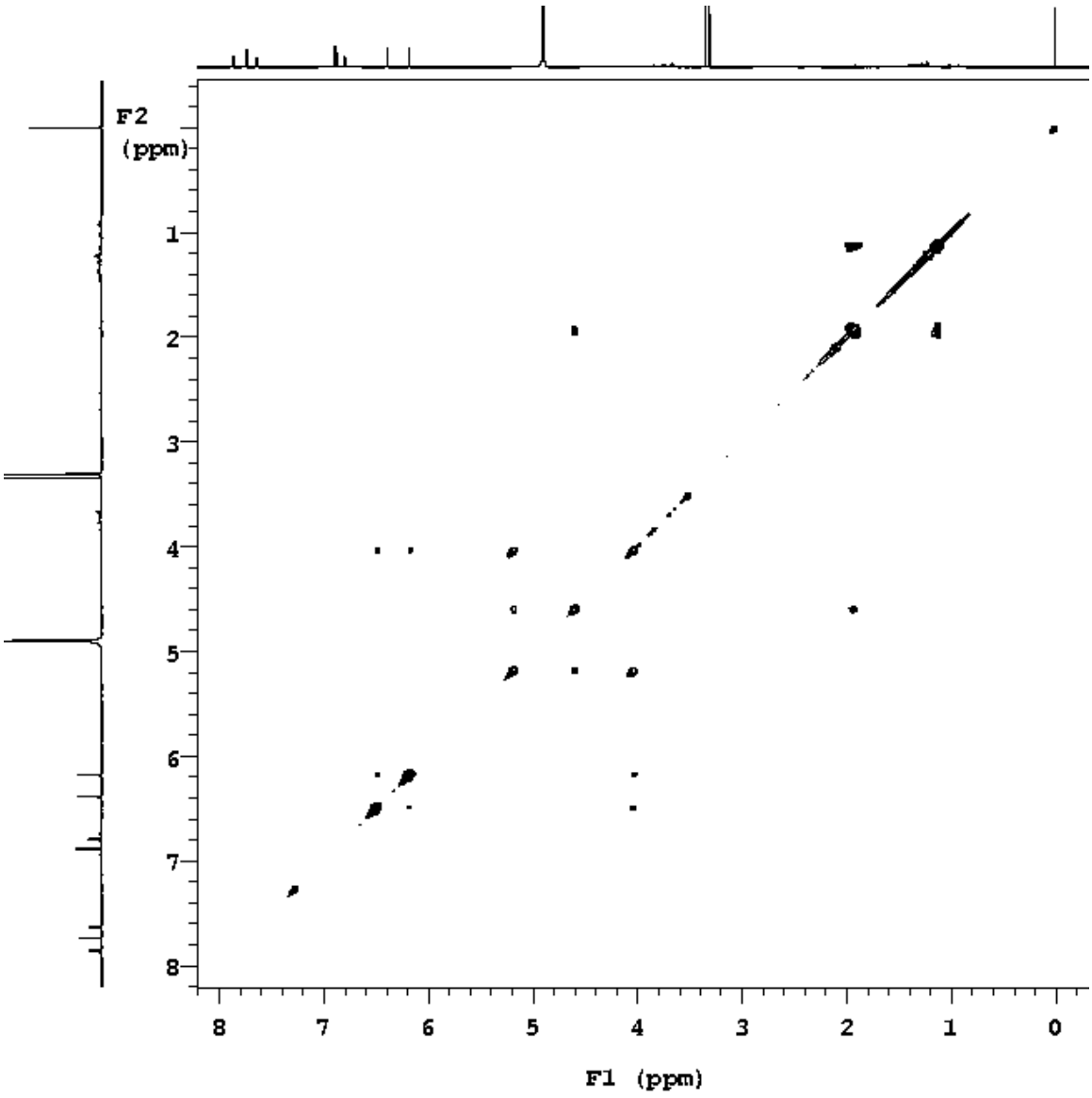

Figure 2-26 The 500 MHz ^{1}H-^{1}H COSY correlation spectrum of Peak A

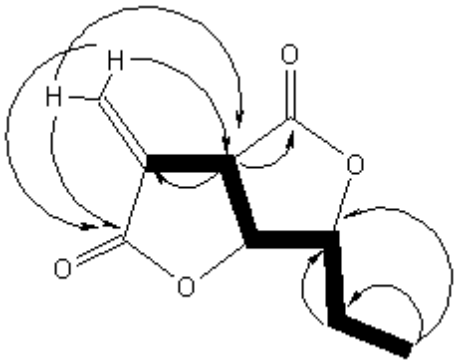

Figure 2-27 Xylobovide from Peak A; arrows indicate proton to carbon correlation through HMBC, bold bonds indicate ^{1}H-^{1}H COSY correlations.

Data from ^{1}H-^{1}H COSY (Figures 2-26 and 2-27) and HMBC (Figures 2-27 and 2-29) experiments confirmed the connectivity of many of the carbons. The HMQC experiment (Figure 2-30) assigned carbon peaks to proton signals, further confirming the structure, and revealed the presence of a carbon peak amid the solvent peaks at δ_C 77.2 (see insert in Figure 2-31).

The ^{13}C NMR (Figure 2-31) in $CDCl_3$ showed 9 carbons: two saturated (δ 9.8, 22.2), one allylic (δ 46.2), two bound with oxygen (δ 77.2, δ84.0), two vinylic (δ 127.4, δ129.7), and two carbonyls (δ 167.4, δ172.1). The NMR data are consistent with the published values for xylobovide (Figure 2-28), isolated in 1997 from *Xylaria Obovata*.[4] Neither FAB-MS nor EI-MS were successful in capturing the molecular ion of this compound.

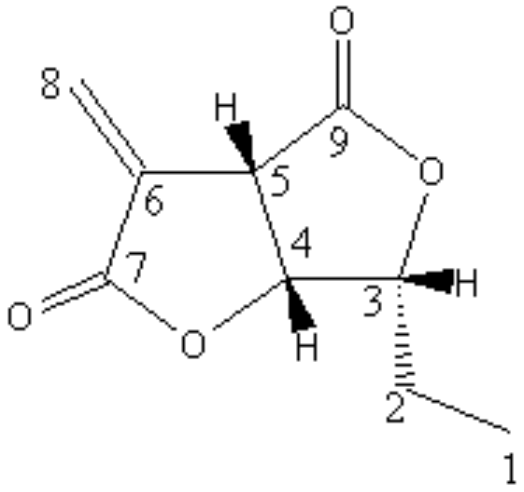

Figure 2-28 Xylobovide

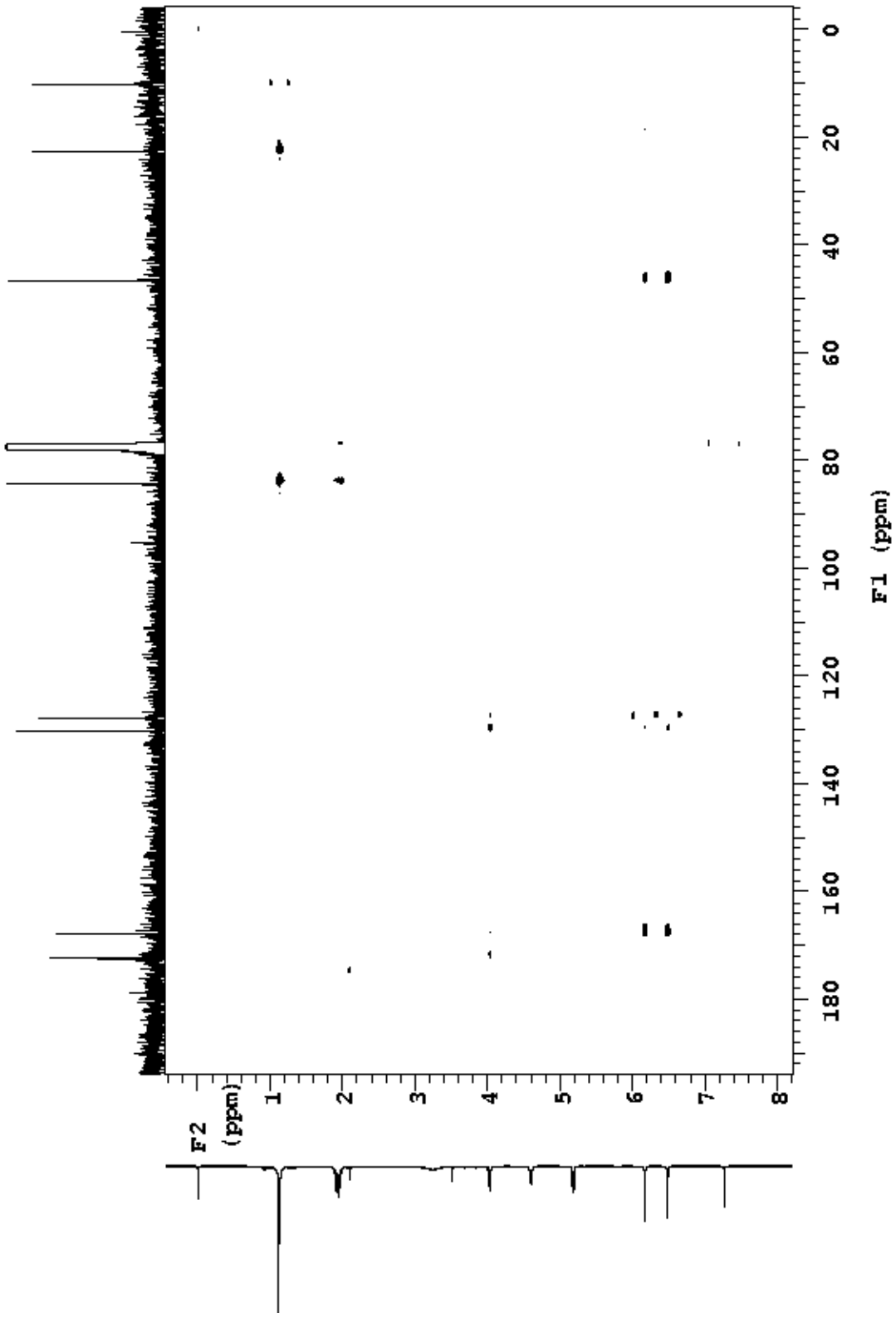

Figure 2-29 500 MHz HMBC long-range correlation spectrum of Peak A in $CDCl_3$

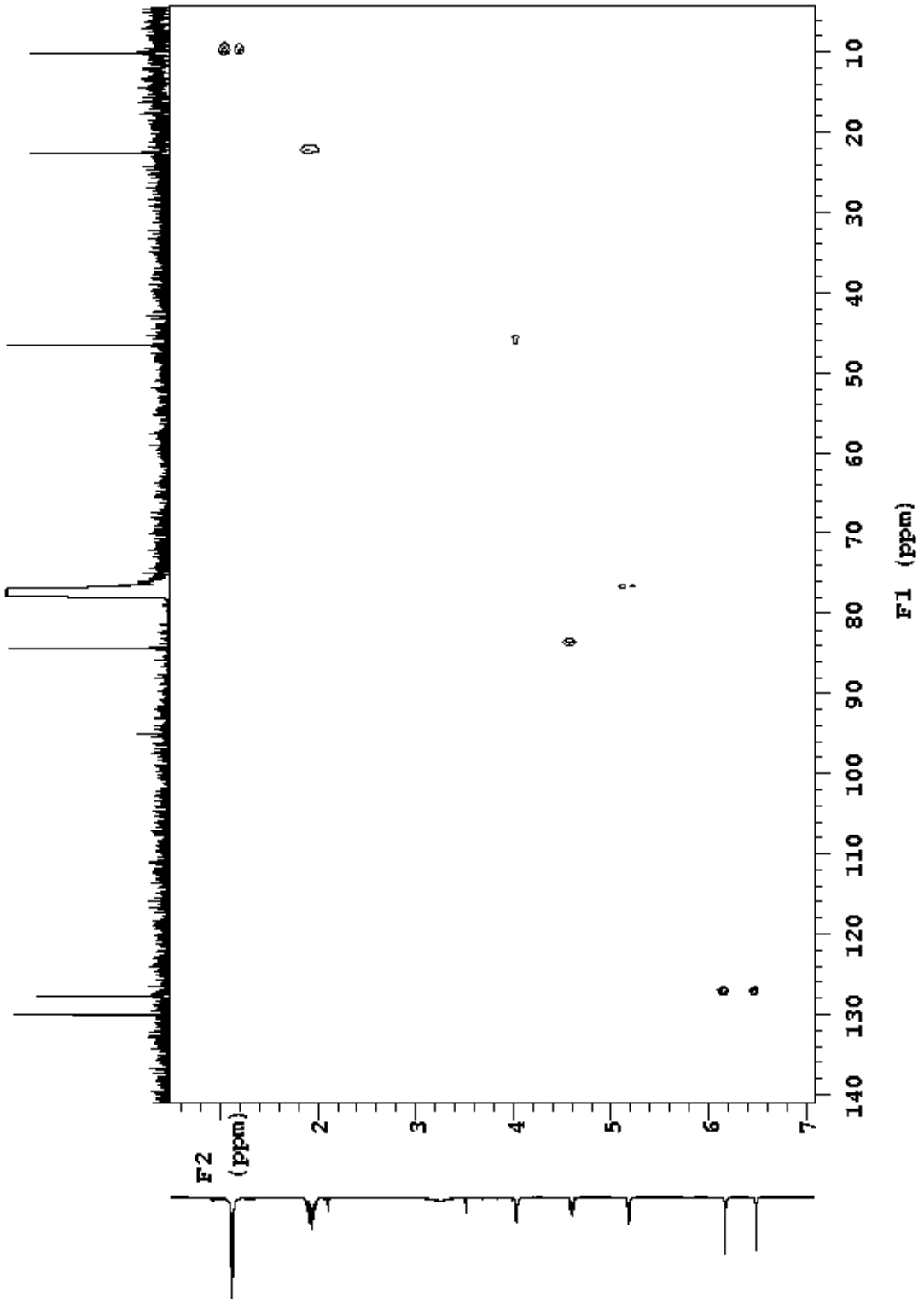

Figure 2-30 500 MHz HMQC correlation spectrum of Peak A in $CDCl_3$

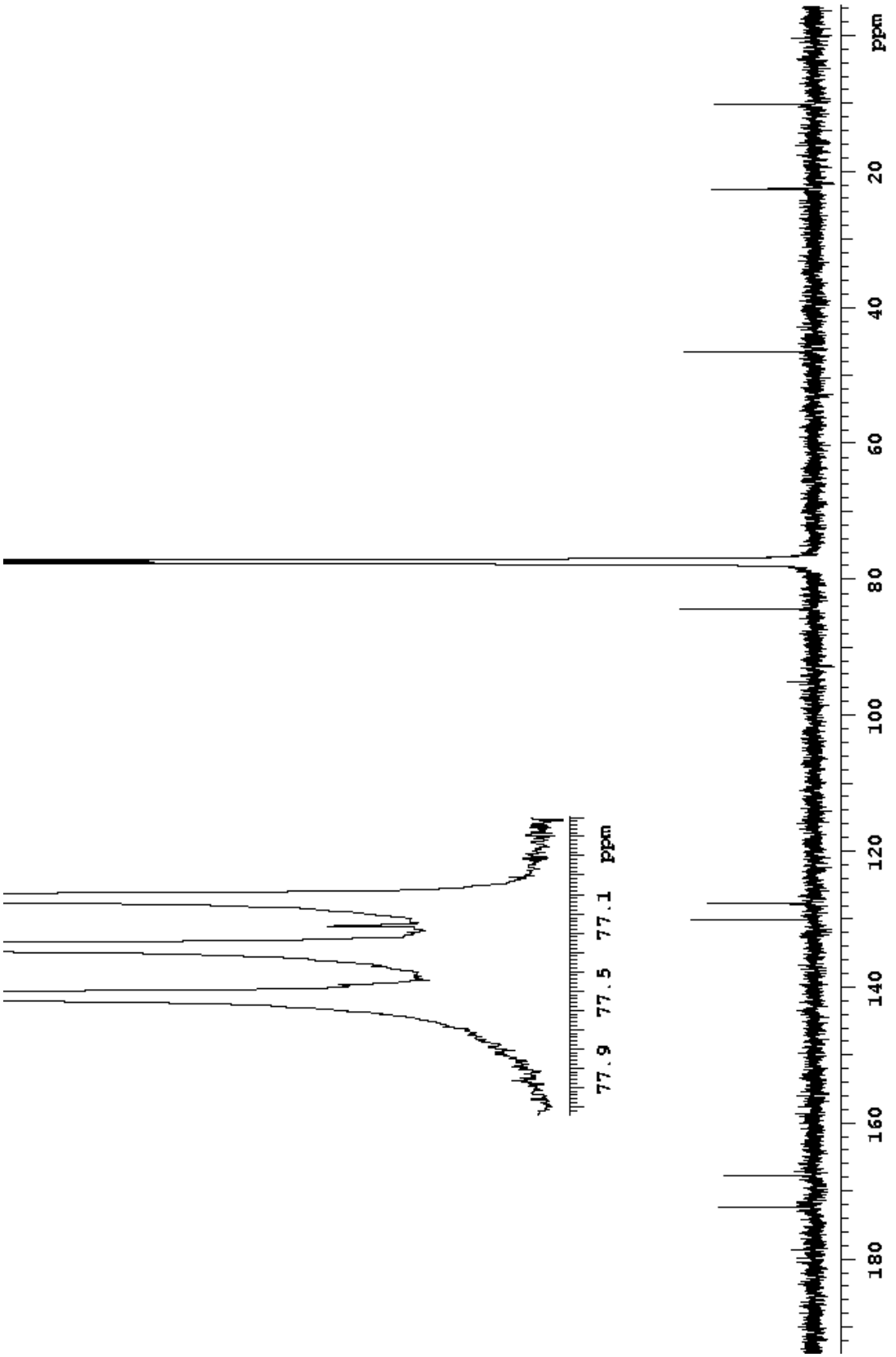

Figure 2-31 500 MHz quantitative ^{13}C NMR spectrum of Peak A in $CDCl_3$

2.6 Discussion

2.6.1 Xylariaceae

The endophyte studied in this treatment was identified as a fungus in the family Xylariaceae, with 18S rDNA sequence similarity to a species of the genus *Xylaria* (GenBank accession # AY315423) and an insert with similarity to a species of the genus *Rosellinia* (GenBank accession # AB014044, also of the family Xylariaceae). Several Xylariaceae have been found to have interesting chemistry, and members of the family are quite often found as endophytes.

2.6.1.1 Xylariaceous Endophytes

Davis et al studied the distribution of Xylariaceous endophytes of liverworts and angiosperms from Jamaica and North Carolina, and found a broad host range for several species of *Xylaria*.[2] Additionally, members of the family Xylariaceae have also been found in conifers, dicots, monocots, ferns, and lycopsids.[5] Endophytic *Xylaria* have been described from nearly every continent, and they are often very closely related to each other. According to Davis, many endophytes obtained from Jamaica, North Carolina, and China[6] all have nearly identical ITS sequences.[2] Interestingly, the present study is the first treatment of a xylariaceous endophyte from Australia.

For survival and propagation, many xylariaceous endophytes are thought to colonize the living plants opportunistically, decomposing the cellulose and lignin for fuel after the plant dies.[2] There is, however, evidence that some Xylariaceae may inhabit plants solely as

endophytes of living plants and decrease in number as the plant begins to decay. There has been no reported benefit to the host in relationship with *Xylaria* endophytes.[2]

2.6.1.2 Chemistry of the Xylareaceae

The chemistry of the xylariaceae has been studied in much detail relative to other fungal families. Roughly 30 years ago, 4,9-dihydroxypeylene, 1,8-dimethoxynaphthalene, rosellinic acid, and diketeopiperazine were discovered in several species. *Rosellinia necatrix* was later found to produce cytochalasin E.[7] To date, the major metabolites discovered (which have been found in roughly a dozen genera) can be grouped as dihydroisocoumarins and derivatives, succinic acid and derivatives, butyrolactones, cytochalasins, sesquiterpene alcohols (punctaporonins), griseofulvin and griseofulvin derivatives, naphthalene derivatives, and long chain fatty acids.[7] The study of metabolites has proved to be invaluable in sorting out the taxonomy of this family.[7]

2.6.2 Cytochalasins

Cytochalasins, of which all are fungal secondary metabolites, are a class of compounds characterized by an 11- or 13-membered macrocyclic ring fused with a highly substituted perhydroisoindol-1-one. Variations on the general cytochalasin skeleton occur in the substituents at C-3 on the perhydroisoindol-1-one ring and the size of the macrocycle.[8] Variation also exists in the type of some substituents on the indole ring and on the macrocycle (see Figure 2-32 for some common cytochalasins).

Cytochalasin A

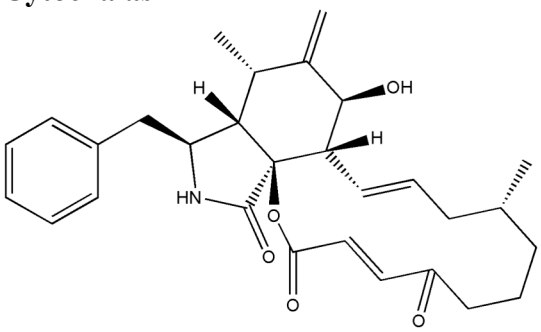

Cytochalasin B

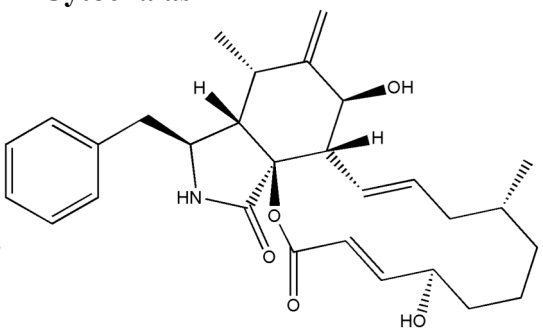

Cytochalasin D

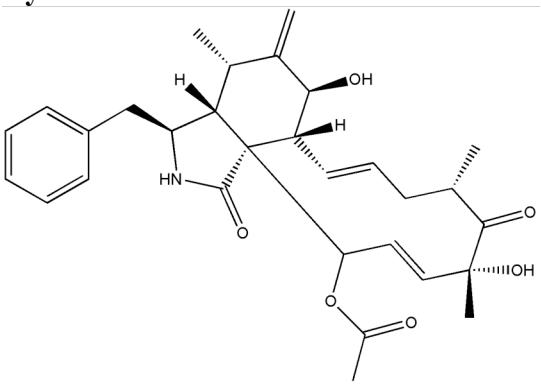

Cytochalasin E

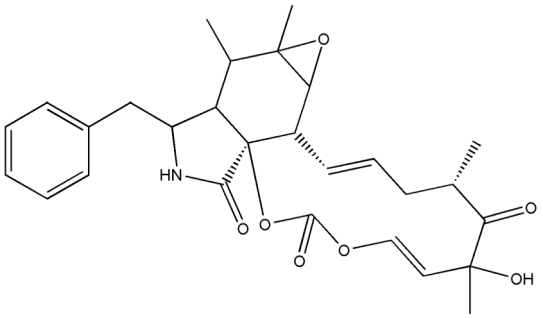

19,20 epoxycythochalasin C

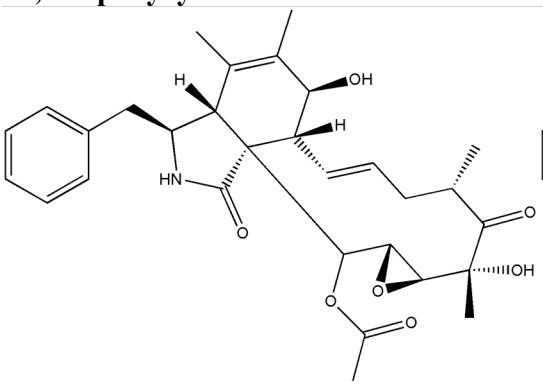

19,20 epoxycytochalasin D

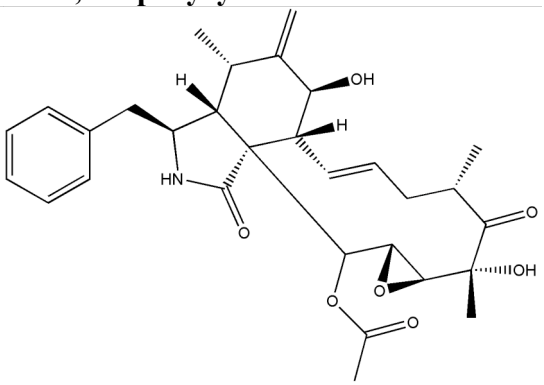

Figure 2-32 Cytochalasins

The Cytochalasins are able to permeate cell membranes and bind to the barbed ends of actin filaments, which inhibits both binding and dissociation of actin subunits at that end. Disruption of actin polymerization causes cells to stop ruffling and translocating, round up, become less stiff, and enucleate.[9] Disruption of actin binding inhibits cytoplasmic cleavage

of mammalian cells.[10] Because of their unique ability to eradicate actin processes, the cytochalasins have helped to elucidate the mechanism of actin polymerization, as well as the role of actin polymerization in various cellular functions.[9, 11, 12]

Most cytochalasins target actin or, less frequently, microtubule formation. Cytochalasins A and B, in addition to binding actin, inhibit monosaccharide transport across the plasma membrane; however, cytochalasins C, D, E, H, and 21,22-dihydro-cytochalasin B do not.[9] Interestingly, cytochalasin E is less effective at binding actin, but inhibits tumor growth in several cancer cell lines through inhibition of angiogenesis.[13]

The first cytochalasin was discovered over thirty years ago, but novel cytochalasins are still studied for their interesting properties and potential as antibiotic and herbicidal agents.[14] The discovery of 19,20-epoxycytochalsin C and D was accomplished in 1997 by analysis of fungal metabolites from the genus *Xylaria*.[3, 4] Several other fungal genera produce cytochalasins, including *Meterrhizium anisopliae* (cytochalasin C), *Drechslera dematoidea*, (cytochalasins A and B), *Zygosporium mansonii* (cytochalasin D), *Aspergillus clavatus* (cytochalasin E),[15] and *Engleromyces goetzei* (19,20 epoxyxytochalasin D).[16]

No studies regarding the activities of 19,20 epoxycytochalasin C and D have been published.

2.6.3 Xylobovide

Xylobovide, an α-methylenebis-γ-butyrolactone, was discovered in 1997 by D Abate et al and was found to be a phytotoxin, inhibiting germination of *Eragrostis tef* seeds at a concentration of 50-100 μg/ml.[4] Xylobovide is structurally related to the compound sporothriolide, which has a hexyl side chain in place of the ethyl side chain on xylobovide.

Krohn et al discovered Sporothriolide in 1994 in a *Sporothrix* sp. from a soil heap in West Borneo, and the compound exhibited strong antibacterial, antifungal, and phytotoxic properties.[17] An experiment was done wherein young pepper seedling plants were sprayed with the fungal pathogen *Botrytis cinerea*. Some were sprayed with a suspension of sporothriolide. Those seedlings that did not receive the sporothriolide treatment exhibited necrosis over 70% of the leaf surfaces, whereas the plants treated with 500ppm sprothriolide did not develop any disease.[17] Obviously, the production of sporothriolide represents a mechanism whereby *Sporothrix* can inhibit the spread of competitor fungi on substrate.

2.7 Methods

2.7.1 Molecular Methods

Total genomic DNA was extracted from fungus grown on M1D using a MoBio UltraClean™ Microbial DNA extraction kit (Cat# 12224-50). DNA was extracted according to instructions. The rDNA was amplified using universal rDNA primers 530F (GTGCCAGCMGCCGCGG) and 1392R (ACGGGCGGTGTGTRC)[18] and *Taq* DNA polymerase with hot start. PCR was performed using 35 cycles of 95°C for 45 sec, 55°C for 45 sec, and 72°C for 1 min 30 sec, with an additional 5-min extension at 72°C after cycling. The PCR product was visualized using 1% agarose gel electrophoresis and quantified densitometrically using a Gel Doc image analysis system (Bio-Rad, Hercules) and Lambda ladder.

PCR product was ligated into pCR 2.1 vector using TA cloning® kit (Invitrogen, Carlsbad, California, USA). Competent XL1 Blue cells were transformed and incubated on ampicillin plates. Transformed colonies were grown for 24 hours and plasmids extracted using QIAprep PCR mini-prep kit (Qiagen, Valencia, California, USA). One colony was found to have insert through EcoR1 restriction digestion, amplified, and sequenced using Big Dyes v.3.1 (Applied Biosystems, Foster City, California, USA) to determine the rDNA sequence. See Appendix, section 3.3 for full rDNA sequence.

2.7.2 Separation and Identification Methods

The ethanol-soluble portion of the extract was dried down and fractionated using a Rainin HPLC system with Dynamax pumps (25 in. head size) and Dynamax UV/Vis

detector. Varian Microsorb MV C18 columns (5μ particle size and 100 Å pore size) with guard were used—size 4.6 x 250mm for analytical separations and 21.4 x 250mm for preparatory separations. HPLC-grade water and acetonitrile with 0.1% trifluoroacetic acid were used as the solvent system. Separations were done isocratically at 46% acetonitrile with 1mL/min and 20mL/min flow rate for analytical and preparatory separations respectively.

Mass spectral data were obtained on a Jeol SX 102A double-focusing reverse geometry high-resolution mass spectrometer using FAB-Xenon methodology in a standard sodiated thioglycerol matrix and standard software unless otherwise indicated. As indicated, some mass spectral data were obtained using an API QSTAR Pulsar i mass spectrometer. The sample was infused at 3 ul/min via a Harvard syringe pump into the API IonSpray Source. A time of flight scan (TOF-MS) was obtained to determine the mass of the compounds present in the sample. Ions of interest were selected for product ion scans (collision induced dissociation, CID) and a fragmentation pattern was obtained.

Gas chromatography was done on a Hewlett-Packard 5890 series II gas chromatograph.

IR data were obtained using a Nicolet Nexus 670 FT-IR infrared spectrometer using the Attenuated Total Reflection (ATR) technique by direct evaporation of solvent with dissolved sample on the diamond.

Crystal data were collected from a single crystal at room temperature on an APEX II CCD detector system using a Bruker FR-591 rotating copper radiation source. Detector-to sample distance was 5.00 cm and the rotation width was 0.5^{o}. APEX2 was used for collecting

data frames, indexing of reflections, and determination of lattice parameters. SAINT was used for integration of the intensity of reflections. SHELXTL was used for data reduction, space group determination, structure determination, structure refinement and structure reporting.

NMR experiments were performed on a Varian INOVA 500, using standard pulse sequences provided by Varian.

2.8 References

(1) Forster, P. I. In *Flora of Australia;* Orchard, A. E., Ed.; CSIRO Publishing: Melbourne, Australia, 1996; Vol. 28, pp 120.

(2) Davis, E. C.; Franklin, J. B.; Shaw, A. J.; Vilgalys, R. *Am. J. Bot.* **2003***, 90*, 1661-1667.

(3) Espada, A.; Rivera-Sagredo, A.; de la Fuente, J.M.; Hueso-Rodriguez, J. A.; Elson, S. W. *Tetrahedron* **1997***, 53*, 6485-6492.

(4) Abate, D.; Abraham, W. R.; Meyer, H. *Phytochemistry* **1997***, 44*, 1443-1448.

(5) Brunner, F.; Petrini, O. *Mycol. Res.* **1992***, 96*, 723-733.

(6) Guo, L. D.; Hyde, K. D.; Liew, E. C. Y. *New Phyt.* **2000***, 147*, 617-630.

(7) Whalley, A. J. S.; Edwards, R. L. *Can J Bot* **1995***, 73*, S802-S810.

(8) Natori, S. *Uakugaku Zasshi* **1983***, 103*, 1109-1128.

(9) Cooper, J. A. *J. Cell Biol.* **1987***, 105*, 1473-1478.

(10) Izawa, Y.; Hirose, T.; Shimizu, T.; Koyama, K.; Natori, S. *Tetrahedron* **1989***, 45*, 2323-2335.

(11) Furukawa, K.; Mattson, M. P. *J. Neurochem.* **1995***, 65*, 1061-1068.

(12) Muscella, A.; Storelli, C.; Marsigliante, S. *J. Cell. Physiol.* **2005**.

(13) Udagawa, T.; Yuan, J.; Panigrahy, D.; Chang, Y. H.; Shah, J.; D'Amato, R. J. *J. Pharmacol. Exp. Ther.* **2000***, 294*, 421-427.

(14) Evidente, A.; Andolfi, A.; Vurro, M.; Zonno, M. C.; Motta, A. *J. Nat. Prod.* **2003***, 66*, 1540-1544.

(15) Fermentek Biotechnology Products. *http://www.fermentek.co.il/products.htm* (accessed 5/13, 2005).

(16) Shibuya, H.; Kitamura, C.; Maehara, S.; Nagahata, M.; Winarno, H.; Simanjuntak, P.; Kim, H. S.; Wataya, Y.; Ohashi, K. *Chem. Pharm. Bull.* **2003***, 51*, 71-74.

(17) Krohn, K.; Ludewig, K.; Aust, H. J.; Draeger, S.; Schulz, B. *J. Antibiot. (Tokyo)* **1994***, 47*, 113-118.

(18) Borneman, J.; Hartin, R. J. *Appl. Environ. Microbiol.* **2000***, 66*, 4356-4360.

3 Isolation of Fungal Secondary Metabolites from an Endophyte of *Acmena graveolens*

3.1 Introduction

Another plant, *Acmena graveolens* (also called Cassowary Satinash), was collected from the Cairns rainforest at the time of the collection of *Alstonia scholaris*. The same preservation and endophyte isolation measures were performed with both plants (see section 2.1). The endophytic fungus labelled 11/17 was isolated from the plant, and its growth medium was found to inhibit the growth of yeast and, to a small extent, HeLa cells.

3.2 Fungus Identification

The rDNA sequence obtained for 11/17 showed perfect homology with several fungal genera of the Hypocreales family (*Fusarium, Gibberella, Cordyceps*, etc), which is consistent with the pink appearance of the mycelium and the compounds isolated (see *Appendix*, section 4.5 for sequence data). ITS sequence data is needed to identify the fungal species.

3.3 Compound Isolation

The fungal mycelia (~0.25 kg) was ground in butanol, and the growth medium (~4 L) was extracted with butanol. The mycelium extract and the media extract were combined. Upon drying of the solvent, most of the material crystallized. The crystals were collected and analyzed using x-ray crystallography.

The crystals were found to partition from the remainder of the material into the water/methanol portion of a water/methanol/chloroform mixture. Roughly 3 g of this water-soluble material was obtained, and roughly 1 g of remaining chloroform-soluble material was obtained. This latter material was in the process of being isolated at the time of publication of this thesis. Activity assays have not yet been performed.

3.4 Structural Determination of Fusaric Acid and Dehydrofusaric Acid

The crystal obtained from the butanol extraction of fungus 11/17 happened to be a co-crystallization of two compounds. Interestingly, both components were very similar, but one component was a zwitterion while the other component was uncharged. The crystal structure is shown in Figure 3-1 (see Appendix 4.2 for tabulated crystal data).

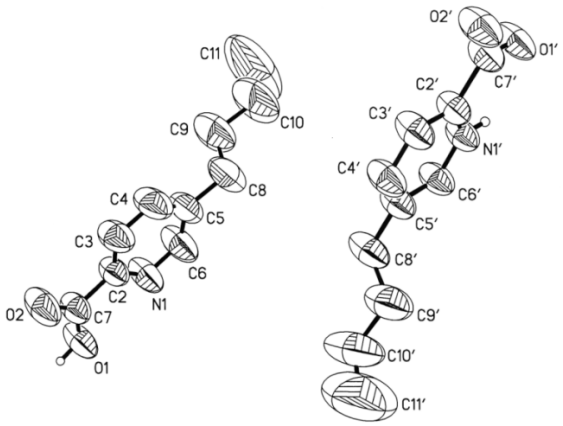

Figure 3-1 Crystal structure ORTEP views of the crystal obtained from fungus 6/35.

The crystal structure data was augmented with GC-MS collision data for dissolved crystal. Gas chromatography was efficacious in separating the two crystal components (see

Figure 3-2). As can be seen in Figure 3-2, there is one major component and one minor component. Collision data was taken of each component, and the mass was determined to be 179 and 177 for the major (11.18 min) and minor (11.00 min) peaks, respectively. The EI collision data for the species of mass 179 matched fusaric acid of the Public/NIST mass spectral database.

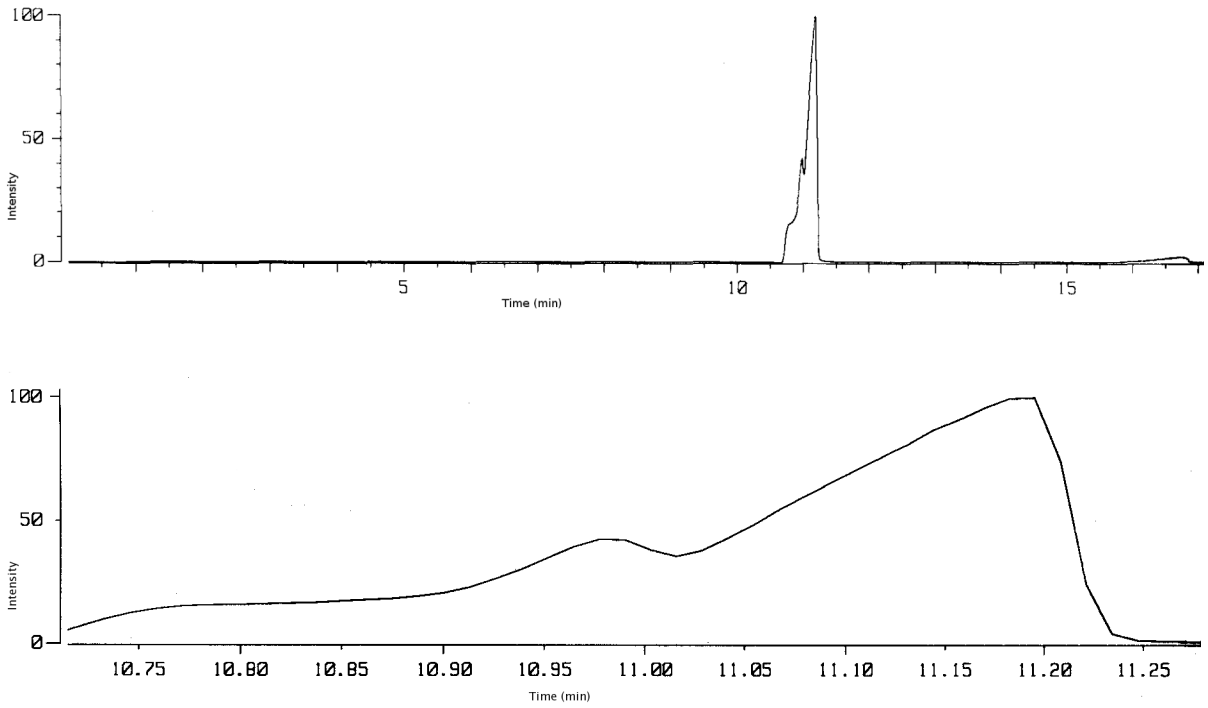

Figure 3-2 Gas chromatograph of crystal obtained from fungus 6/35.

The collision data for the peak of mass 177 showed a near identical fragmentation pattern to that of m/z 179, with a two mass unit difference on many ions. Because the crystal data and GC-MS data showed conclusively the components of the crystal to be fusaric acid and dehydrofusaric acid (which are known compounds), very little more experimentation was done. The ^{1}H NMR and ^{13}C NMR data for the dissolved crystal are shown in Figures 3-5

and 3-6. HPLC was performed (see *methods*, section 2.7) on the combined extract, with a methanol-water gradient of 37% methanol to 100% methanol over 15 min (see Figure 3-7). As noted on the HPLC profile, fusaric acid and dehydrofusaric acid eluted together early.

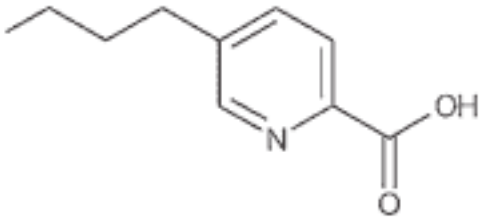

Figure 3-3 Fusaric acid

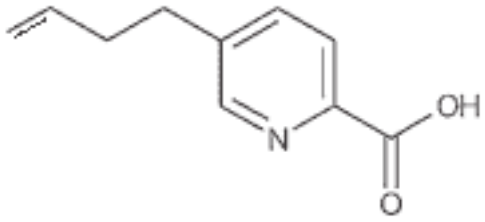

Figure 3-4 Dehydrofusaric acid

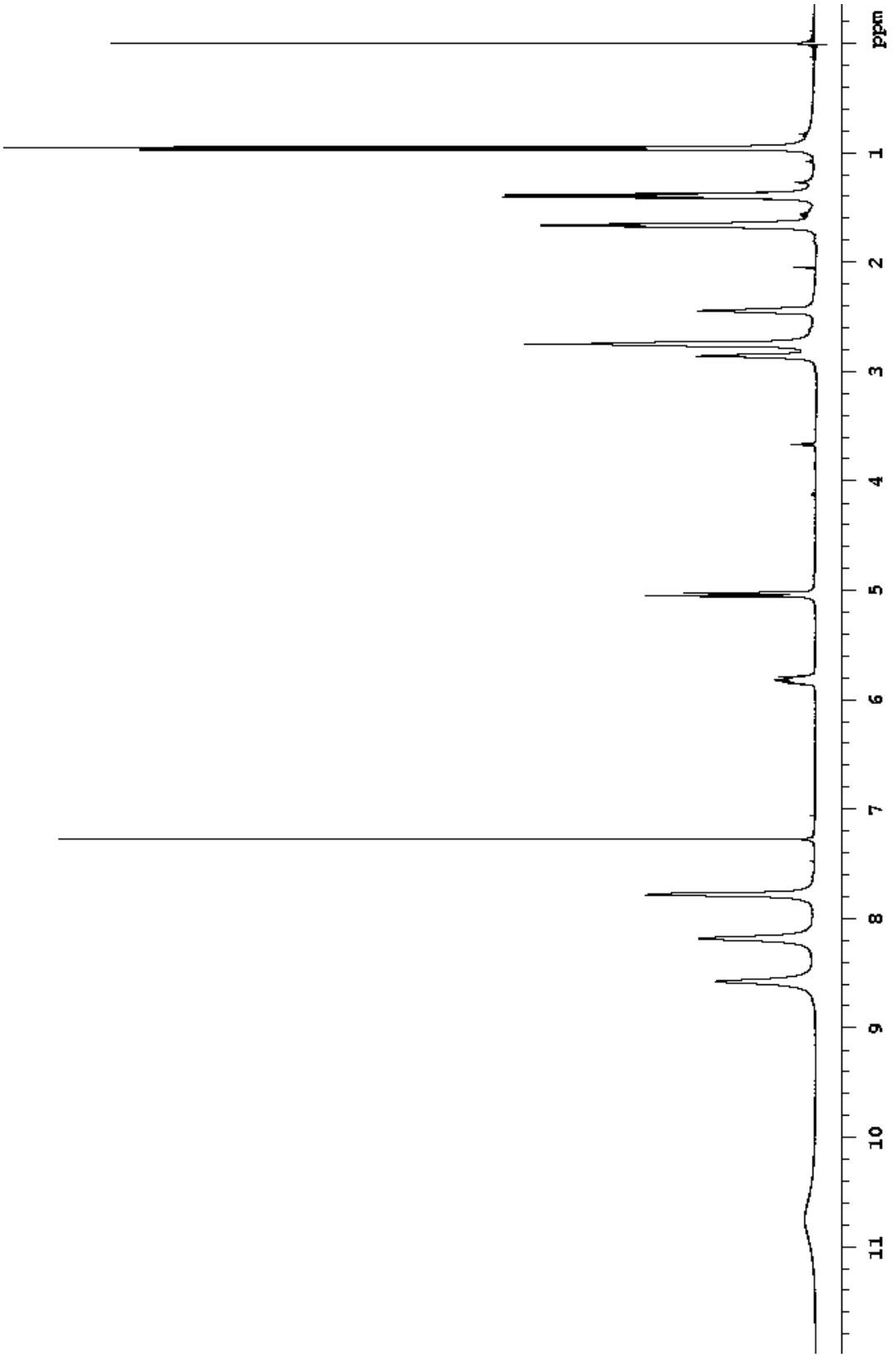

Figure 3-5 500 MHz ^{1}H NMR spectrum of fusaric acid and dehydrofusaric acid.

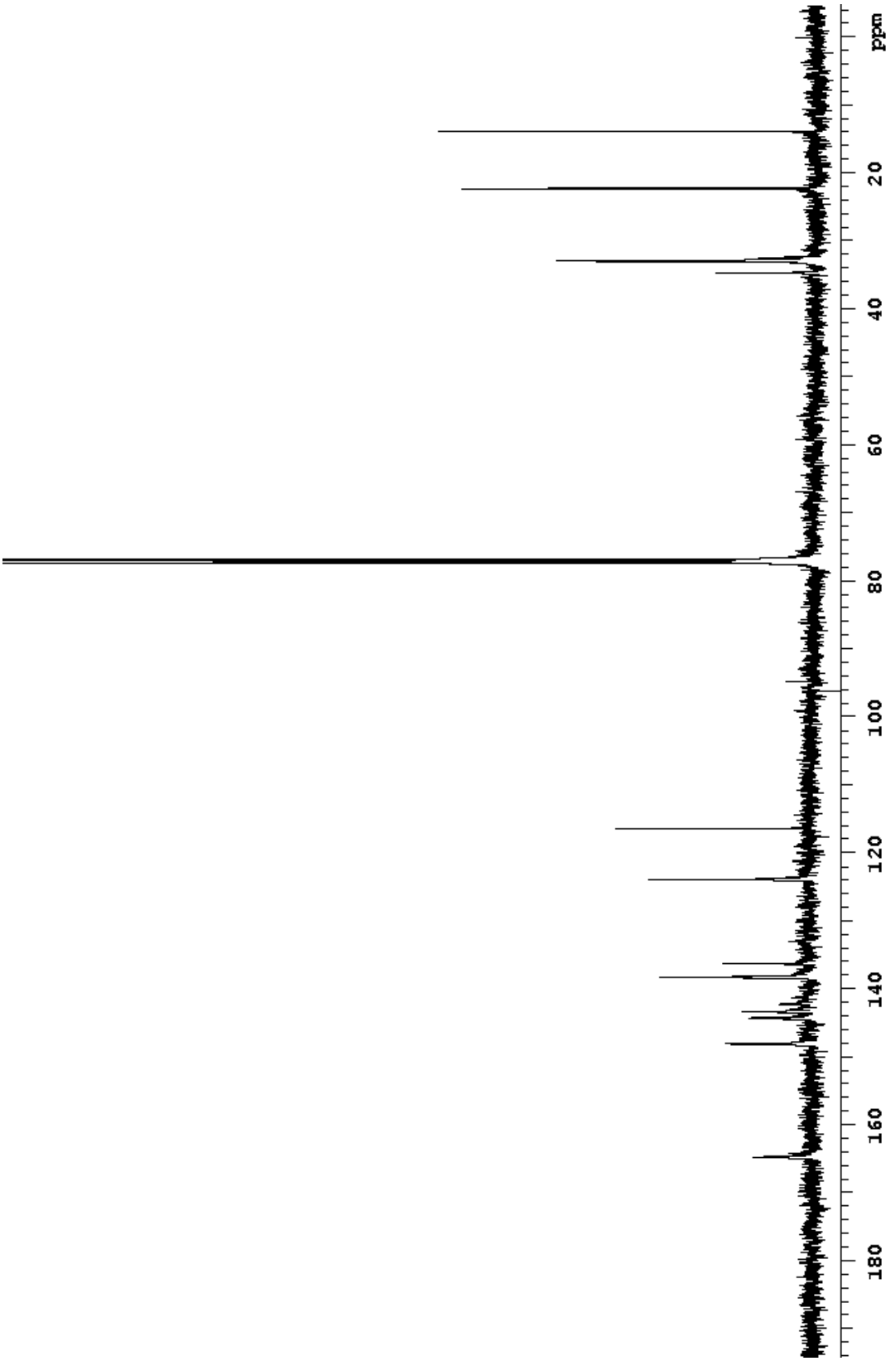

Figure 3-6 500 MHZ ^{13}C NMR spectrum of fusaric acid and dehydrofusaric acid.

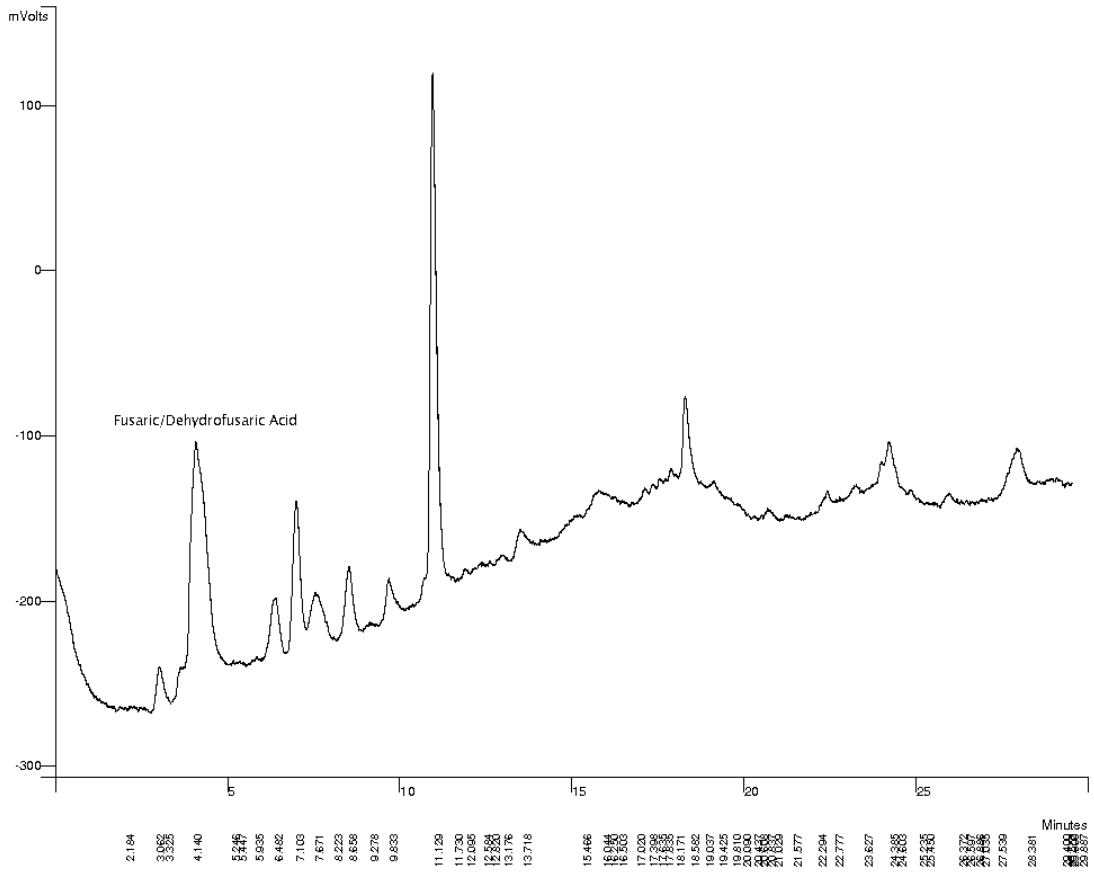

Figure 3-7 HPLC profile of combined mycelia/liquid butanol extract of fungus 11/17; 37%→100% methanol gradient over 15 min.

3.5 Discussion

Fusarium fungi are common cereal pathogens and are capable of producing several highly toxic and sometimes problematic compounds, trichothecenes being the most salient. Among these, deoxynivalenol, T-2 toxin, HT-2 toxin, and nivalenol are known to cause emesis and anorexia in animals. These effects are thought to occur through action on serotonergic receptors in the central or peripheral nervous system.[1] Fusaric acid is a non-

trichothecene compound commonly produced by the *Fusarium* fungi; however, its effects are targeted toward competing bacterial endophytes as well as diverting animal grazing. [2] Fusaric acid greatly inhibits the growth of beneficial endophytic bacteria such as *Bacillus subtilis* and *Bacillus mojavensis* in corn plants, [3] which poses a problem for the engineering of competitive *Bacillus* endophytes for cereal agriculture. Interestingly, fusaric acid also has anti-hypertensive effects through dopamine beta-hydroxylase inhibition and peripheral vascular resistance reduction in humans, and it was also included in several clinical trials.[4,5]

3.6 References

(1) Rotter BA, Prelusky DB, Pestka JJ. Toxicology of desoxynivalenol (Vomitoxin). J Toxicol Environ Health. **1996**, 48: 1-34.

(2) Smith, T. K.; MacDonald, E. J. J. Anim. Sci. **1991**, 69, 2044-2049.

(3) Bacon, C. W.; Hinton, D. M.; Porter, J. K.; Glenn, A. E.; Kuldau, G. Can. J. Bot. **2004**, 82, 878-885.

(4) Terasawa, F.; Hidaka, H. Jpn. Circ. J. **1976**, 40, 785-791.

(5) Terasawa, F.; Ying, L. H.; Suzuki, T. Jpn. Circ. J. **1976**, 40, 1025-1031.

4 Appendix

4.1 Crystal Structure Data for Peak F

Table 4-1 Crystal data and structure refinement for Peak F_0m.

Identification code	nh1_0m	
Empirical formula	C30 H37 N O7	
Formula weight	523.61	
Temperature	297(2) K	
Wavelength	1.54178 Å	
Crystal system	Orthorhombic	
Space group	P2(1)2(1)2(1)	
Unit cell dimensions	a = 7.7737(4) Å	a= 90°.
	b = 12.8217(7) Å	b= 90°.
	c = 29.1614(18) Å	g = 90°.
Volume	2906.6(3) $Å^3$	
Z	4	
Density (calculated)	1.197 Mg/m^3	
Absorption coefficient	0.691 mm^{-1}	
F(000)	1120	
Crystal size	0.20 x 0.04 x 0.01 mm^3	
Theta range for data collection	3.77 to 42.20°.	
Index ranges	-6<=h<=6, -11<=k<=9, -24<=l<=25	
Reflections collected	5824	
Independent reflections	1878 [R(int) = 0.0470]	
Completeness to theta = 42.20°	97.0 %	
Absorption correction	Semi-empirical from equivalents	
Max. and min. transmission	0.9931 and 0.8741	
Refinement method	Full-matrix least-squares on F^2	
Data / restraints / parameters	1878 / 0 / 355	
Goodness-of-fit on F^2	0.980	
Final R indices [I>2sigma(I)]	R1 = 0.0348, wR2 = 0.0703	
R indices (all data)	R1 = 0.0557, wR2 = 0.0755	
Absolute structure parameter	0.6(3)	
Extinction coefficient	0.0015(2)	

Largest diff. peak and hole 0.100 and -0.098 e.Å^{-3}

Table 4-2 Atomic coordinates (x 10^4) and equivalent isotropic displacement parameters (Å^{2}x 10^3) for NH1_0m. U(eq) is defined as one third of the trace of the orthogonalized U^{ij} tensor.

	x	y	z	U(eq)
C(1)	7183(9)	8400(4)	593(3)	64(2)
C(3)	6165(7)	8309(4)	1363(2)	71(2)
C(4)	8041(7)	8706(4)	1388(2)	63(1)
C(5)	9173(8)	7882(5)	1594(2)	77(2)
C(6)	10271(8)	7298(4)	1357(2)	69(2)
C(7)	10586(7)	7539(4)	862(2)	64(1)
C(8)	10373(7)	8703(3)	761(2)	58(1)
C(9)	8506(7)	9008(3)	884(2)	53(1)
C(10)	4770(7)	9054(4)	1522(2)	96(2)
C(11)	8856(7)	7725(4)	2102(2)	115(2)
C(12)	11202(7)	6369(4)	1543(2)	109(2)
C(13)	11019(8)	8961(4)	290(2)	63(1)
C(14)	12338(7)	9563(4)	196(2)	67(2)
C(15)	13082(6)	9745(3)	-272(2)	80(2)
C(16)	12314(7)	10683(4)	-519(2)	69(1)
C(17)	10456(9)	10469(4)	-625(2)	72(2)
C(18)	9005(7)	11163(4)	-456(2)	74(2)
C(19)	9075(7)	11165(4)	61(2)	69(2)
C(20)	7897(7)	10540(4)	337(2)	68(2)
C(21)	8154(7)	10199(4)	820(2)	67(2)
C(22)	13280(7)	10901(4)	-967(2)	100(2)
C(23)	9194(7)	12252(4)	-654(2)	110(2)
C(24)	9251(11)	11418(5)	1378(2)	85(2)
C(25)	10827(8)	11885(4)	1552(2)	115(2)
C(1')	4701(8)	9227(8)	2037(2)	87(2)
C(2')	4030(10)	8467(6)	2308(4)	138(3)
C(3')	4020(13)	8594(8)	2775(5)	177(4)

C(4')	4626(14)	9474(13)	2970(3)	191(4)
C(5')	5260(10)	10215(8)	2701(5)	178(4)
C(6')	5317(9)	10112(6)	2231(4)	127(3)
N(2)	5956(8)	8072(4)	881(2)	80(2)
O(1)	7214(4)	8272(2)	181(1)	80(1)
O(2)	12304(4)	7203(2)	743(1)	75(1)
O(3)	10077(5)	9699(3)	-856(1)	96(1)
O(4)	7423(4)	10728(3)	-609(1)	107(1)
O(5)	7617(5)	11654(3)	271(1)	105(1)
O(6)	9592(4)	10762(3)	1020(1)	72(1)
O(7)	7816(7)	11553(3)	1513(2)	119(2)

Table 4-3 Bond lengths [Å] and angles [°] for NH1_0m.

C(1)-O(1)	1.212(6)	C(24)-O(6)	1.367(6)
C(1)-N(2)	1.339(6)	C(24)-C(25)	1.454(7)
C(1)-C(9)	1.545(6)	C(1')-C(6')	1.355(7)
C(3)-N(2)	1.447(6)	C(1')-C(2')	1.358(7)
C(3)-C(10)	1.518(6)	C(2')-C(3')	1.373(9)
C(3)-C(4)	1.547(6)	C(3')-C(4')	1.348(9)
C(4)-C(5)	1.501(6)	C(4')-C(5')	1.327(9)
C(4)-C(9)	1.563(5)	C(5')-C(6')	1.376(8)
C(5)-C(6)	1.328(6)		
C(5)-C(11)	1.515(6)	O(1)-C(1)-N(2)	126.5(6)
C(6)-C(12)	1.496(6)	O(1)-C(1)-C(9)	126.8(6)
C(6)-C(7)	1.496(6)	N(2)-C(1)-C(9)	106.7(6)
C(7)-O(2)	1.446(5)	N(2)-C(3)-C(10)	110.4(5)
C(7)-C(8)	1.532(5)	N(2)-C(3)-C(4)	102.8(5)
C(8)-C(13)	1.499(6)	C(10)-C(3)-C(4)	116.8(5)
C(8)-C(9)	1.545(6)	C(5)-C(4)-C(3)	109.9(4)
C(9)-C(21)	1.562(6)	C(5)-C(4)-C(9)	114.5(4)
C(10)-C(1')	1.519(6)	C(3)-C(4)-C(9)	104.7(4)
C(13)-C(14)	1.313(5)	C(6)-C(5)-C(4)	124.5(5)
C(14)-C(15)	1.500(6)	C(6)-C(5)-C(11)	122.5(6)
C(15)-C(16)	1.524(5)	C(4)-C(5)-C(11)	112.9(6)
C(16)-C(17)	1.503(6)	C(5)-C(6)-C(12)	124.8(6)
C(16)-C(22)	1.532(5)	C(5)-C(6)-C(7)	119.4(5)
C(17)-O(3)	1.230(5)	C(12)-C(6)-C(7)	115.8(5)
C(17)-C(18)	1.520(7)	O(2)-C(7)-C(6)	108.8(5)
C(18)-O(4)	1.423(5)	O(2)-C(7)-C(8)	110.1(4)
C(18)-C(19)	1.508(6)	C(6)-C(7)-C(8)	111.7(4)
C(18)-C(23)	1.518(6)	C(13)-C(8)-C(7)	110.8(4)
C(19)-O(5)	1.433(6)	C(13)-C(8)-C(9)	118.2(4)
C(19)-C(20)	1.459(6)	C(7)-C(8)-C(9)	107.7(4)
C(20)-O(5)	1.458(5)	C(8)-C(9)-C(1)	111.7(4)
C(20)-C(21)	1.489(6)	C(8)-C(9)-C(21)	112.6(4)
C(21)-O(6)	1.453(5)	C(1)-C(9)-C(21)	108.1(4)
C(24)-O(7)	1.195(6)	C(8)-C(9)-C(4)	111.9(4)

C(1)-C(9)-C(4)	103.8(4)	O(5)-C(20)-C(19)	58.8(3)
C(21)-C(9)-C(4)	108.2(4)	O(5)-C(20)-C(21)	115.6(4)
C(3)-C(10)-C(1')	114.8(5)	C(19)-C(20)-C(21)	126.8(5)
C(14)-C(13)-C(8)	125.7(5)	O(6)-C(21)-C(20)	109.7(4)
C(13)-C(14)-C(15)	125.6(5)	O(6)-C(21)-C(9)	107.7(4)
C(14)-C(15)-C(16)	113.7(4)	C(20)-C(21)-C(9)	115.0(4)
C(17)-C(16)-C(15)	109.2(4)	O(7)-C(24)-O(6)	121.4(6)
C(17)-C(16)-C(22)	109.2(4)	O(7)-C(24)-C(25)	127.8(7)
C(15)-C(16)-C(22)	110.8(4)	O(6)-C(24)-C(25)	110.8(6)
O(3)-C(17)-C(16)	119.3(5)	C(6')-C(1')-C(2')	119.5(6)
O(3)-C(17)-C(18)	118.0(6)	C(6')-C(1')-C(10)	121.6(9)
C(16)-C(17)-C(18)	122.6(5)	C(2')-C(1')-C(10)	118.9(9)
O(4)-C(18)-C(19)	110.3(5)	C(1')-C(2')-C(3')	119.6(8)
O(4)-C(18)-C(23)	108.9(5)	C(4')-C(3')-C(2')	121.0(9)
C(19)-C(18)-C(23)	112.1(5)	C(5')-C(4')-C(3')	118.7(11)
O(4)-C(18)-C(17)	108.0(5)	C(4')-C(5')-C(6')	122.1(9)
C(19)-C(18)-C(17)	107.4(5)	C(1')-C(6')-C(5')	119.0(7)
C(23)-C(18)-C(17)	110.0(5)	C(1)-N(2)-C(3)	117.7(6)
O(5)-C(19)-C(20)	60.5(3)	C(19)-O(5)-C(20)	60.6(3)
O(5)-C(19)-C(18)	113.5(5)	C(24)-O(6)-C(21)	117.6(4)
C(20)-C(19)-C(18)	121.8(5)		

Table 4-4 Anisotropic displacement parameters ($Å^2 x\ 10^3$) for NH1_0m. The anisotropic displacement factor exponent takes the form: $-2p^2[\ h^2\ a^{*2}U^{11} + ...\ + 2\ h\ k\ a^*\ b^*\ U^{12}\ ]$

	U^{11}	U^{22}	U^{33}	U^{23}	U^{13}	U^{12}
C(1)	57(5)	66(3)	68(5)	-3(4)	1(6)	2(3)
C(3)	54(5)	98(4)	61(5)	-8(3)	1(4)	-7(4)
C(4)	60(4)	75(3)	54(4)	-6(3)	-3(3)	-8(3)
C(5)	79(5)	101(4)	50(5)	6(4)	-1(4)	-4(4)
C(6)	72(4)	72(4)	61(5)	3(4)	1(4)	0(4)
C(7)	50(4)	68(4)	73(5)	-17(3)	1(3)	1(3)
C(8)	61(4)	56(4)	58(4)	-9(3)	-13(3)	7(3)
C(9)	48(4)	57(3)	54(4)	-8(3)	-5(3)	4(3)
C(10)	67(4)	138(5)	82(6)	-4(4)	6(4)	-6(4)
C(11)	112(5)	159(5)	73(5)	16(4)	1(4)	1(5)
C(12)	128(5)	102(4)	99(5)	23(3)	-15(4)	19(4)
C(13)	68(4)	67(3)	54(4)	-8(3)	-11(4)	7(3)
C(14)	58(4)	68(3)	74(5)	-3(3)	-4(4)	-4(3)
C(15)	68(4)	91(4)	80(5)	15(3)	13(4)	12(3)
C(16)	51(4)	73(4)	83(4)	2(3)	-15(4)	-6(3)
C(17)	89(6)	75(4)	51(4)	0(3)	-3(4)	-14(5)
C(18)	52(5)	90(4)	80(5)	-3(4)	-8(4)	1(4)
C(19)	54(4)	82(4)	73(5)	-12(4)	0(4)	17(4)
C(20)	62(4)	53(3)	90(5)	-6(3)	1(4)	10(3)
C(21)	69(5)	78(4)	54(5)	-3(3)	-2(3)	7(4)
C(22)	78(4)	132(4)	90(5)	40(4)	12(4)	1(4)
C(23)	101(5)	106(4)	123(5)	43(4)	-11(4)	14(4)
C(24)	109(7)	71(4)	76(5)	-8(4)	11(5)	-17(5)
C(25)	139(6)	119(4)	86(5)	-27(3)	-9(5)	-45(5)
C(1')	71(4)	127(6)	61(6)	-8(6)	14(4)	-23(4)
C(2')	166(7)	151(7)	97(8)	-26(6)	59(6)	-53(6)
C(3')	229(10)	179(9)	125(11)	1(7)	76(8)	-51(8)
C(4')	217(11)	270(12)	86(8)	-9(9)	53(7)	-76(10)
C(5')	183(8)	246(11)	104(9)	-80(8)	44(7)	-93(8)

C(6')	137(6)	129(6)	115(9)	-29(5)	38(6)	-54(5)
N(2)	61(4)	116(4)	64(5)	-20(3)	-2(4)	-29(4)
O(1)	87(3)	103(2)	49(2)	-16(2)	-3(3)	-12(2)
O(2)	78(3)	75(2)	71(2)	-3(2)	-1(2)	16(2)
O(3)	85(3)	120(3)	82(3)	-16(2)	2(2)	-25(3)
O(4)	63(3)	166(4)	93(3)	4(3)	-15(2)	-10(3)
O(5)	103(3)	96(3)	116(3)	8(2)	14(3)	28(3)
O(6)	79(3)	71(2)	66(3)	-20(2)	-3(2)	-2(2)
O(7)	139(4)	90(3)	128(4)	-34(2)	53(3)	-19(3)

Table 4-5 Hydrogen coordinates (x 10^4) and isotropic displacement parameters ($Å^2$x 10^3) for NH1_0m.

	x	y	z	U(eq)
H(3)	6074	7660	1539	85
H(4)	8082	9332	1581	75
H(7)	9758	7147	676	76
H(8)	11119	9074	977	70
H(10A)	3664	8787	1422	115
H(10B)	4946	9722	1373	115
H(11A)	9569	7168	2213	172
H(11B)	7668	7552	2151	172
H(11C)	9128	8356	2264	172
H(12A)	10873	6260	1857	164
H(12B)	12420	6488	1527	164
H(12C)	10911	5764	1366	164
H(13)	10434	8669	43	76
H(14)	12857	9907	440	80
H(15A)	12895	9127	-457	96
H(15B)	14314	9845	-243	96
H(16)	12393	11297	-320	83
H(19)	10197	11318	199	83
H(20)	7126	10092	159	82

H(21)	7116	10377	994	80
H(22A)	13296	10282	-1151	150
H(22B)	14438	11109	-898	150
H(22C)	12710	11451	-1131	150
H(23A)	9194	12213	-983	165
H(23B)	10256	12553	-551	165
H(23C)	8250	12678	-554	165
H(25A)	10551	12390	1783	172
H(25B)	11427	12221	1305	172
H(25C)	11545	11351	1681	172
H(2')	3579	7865	2177	166
H(3')	3589	8065	2960	213
H(4')	4601	9560	3286	229
H(5')	5678	10823	2834	213
H(6')	5771	10641	2050	153
H(2A)	12347	7075	467	112
H(4A)	7616	10201	-760	161
H(2)	5100(60)	7740(30)	792(16)	61(19)

4.2 Crystal Structure Data for Fusaric Acid and Dehydrofusaric Acid

Table 4-6. Crystal data and structure refinement for NL2_0m.

Identification code	nl2_0m	
Empirical formula	C20 H24 N2 O4	
Formula weight	356.41	
Temperature	273(2) K	
Wavelength	1.54178 Å	
Crystal system	Monoclinic	
Space group	P2(1)/n	
Unit cell dimensions	a = 12.097(2) Å	a= 90°.
	b = 10.399(2) Å	b= 109.26(3)°.
	c = 17.131(3) Å	g = 90°.
Volume	2034.3(7) $Å^3$	
Z	4	
Density (calculated)	1.164 Mg/m^3	
Absorption coefficient	0.664 mm^{-1}	
F(000)	760	
Crystal size	0.40 x 0.35 x 0.20 mm^3	
Theta range for data collection	5.43 to 50.49°.	
Index ranges	-12<=h<=12, -10<=k<=8, -17<=l<=17	
Reflections collected	7031	
Independent reflections	2119 [R(int) = 0.0163]	
Completeness to theta = 50.49°	99.3 %	
Absorption correction	None	
Refinement method	Full-matrix least-squares on F^2	
Data / restraints / parameters	2119 / 0 / 241	
Goodness-of-fit on F^2	1.035	
Final R indices [I>2sigma(I)]	R1 = 0.0600, wR2 = 0.1849	
R indices (all data)	R1 = 0.0651, wR2 = 0.1935	
Largest diff. peak and hole	0.241 and -0.144 $e.Å^{-3}$	

Table 4-7. Atomic coordinates (x 10^4) and equivalent isotropic displacement parameters ($Å^2$x 10^3) for NL2_0m. U(eq) is defined as one third of the trace of the orthogonalized U^{ij} tensor.

	x	y	z	U(eq)
C(2)	2816(2)	2065(3)	9973(2)	79(1)
N(1)	2690(2)	804(3)	9873(2)	109(1)
O(1)	4628(2)	1697(2)	11000(2)	104(1)
C(3)	2030(3)	2901(3)	9471(2)	106(1)
O(2)	4034(2)	3693(2)	10749(2)	128(1)
C(4)	1063(3)	2433(4)	8851(2)	118(1)
C(11)	-3094(10)	-230(16)	7614(6)	376(9)
C(5)	907(3)	1135(4)	8739(2)	104(1)
C(6)	1746(3)	391(4)	9266(3)	125(2)
C(7)	3885(3)	2567(3)	10620(2)	83(1)
C(8)	-126(3)	548(5)	8069(3)	136(2)
C(9)	-1189(4)	517(8)	8259(4)	207(3)
C(10)	-2205(5)	-63(11)	7558(5)	274(6)
N(1')	-1288(2)	1704(2)	3208(1)	71(1)
C(2')	-1595(2)	2918(2)	2968(2)	70(1)
O(1')	-3333(2)	2105(2)	2034(1)	94(1)
C(3')	-858(3)	3881(3)	3371(2)	84(1)
O(2')	-3018(2)	4218(2)	2039(1)	101(1)
C(4')	151(3)	3591(3)	4012(2)	88(1)
C(11')	4728(7)	1756(11)	5509(6)	311(6)
C(5')	443(2)	2331(3)	4256(2)	78(1)
C(6')	-319(2)	1394(3)	3820(2)	76(1)
C(7')	-2753(3)	3113(3)	2282(2)	79(1)
C(8')	1521(3)	1991(3)	4963(2)	99(1)
C(9')	2609(3)	1936(5)	4747(3)	133(2)
C(10')	3719(4)	1635(5)	5543(4)	176(3)

Table 4-8. Bond lengths [Å] and angles [°] for NL2_0m.

		C(2)-N(1)-C(6)	116.8(3)
C(2)-N(1)	1.324(4)	C(2)-C(3)-C(4)	119.8(3)
C(2)-C(3)	1.364(4)	C(5)-C(4)-C(3)	119.8(3)
C(2)-C(7)	1.492(4)	C(6)-C(5)-C(4)	115.6(3)
N(1)-C(6)	1.336(4)	C(6)-C(5)-C(8)	121.5(4)
O(1)-C(7)	1.290(4)	C(4)-C(5)-C(8)	122.9(4)
C(3)-C(4)	1.383(5)	N(1)-C(6)-C(5)	126.5(4)
O(2)-C(7)	1.195(4)	O(2)-C(7)-O(1)	123.8(3)
C(4)-C(5)	1.368(5)	O(2)-C(7)-C(2)	121.4(3)
C(11)-C(10)	1.125(11)	O(1)-C(7)-C(2)	114.8(3)
C(5)-C(6)	1.356(5)	C(9)-C(8)-C(5)	114.5(4)
C(5)-C(8)	1.519(5)	C(8)-C(9)-C(10)	112.3(5)
C(8)-C(9)	1.428(7)	C(11)-C(10)-C(9)	122.4(9)
C(9)-C(10)	1.532(7)	C(6')-N(1')-C(2')	123.6(2)
N(1')-C(6')	1.330(4)	N(1')-C(2')-C(3')	117.8(2)
N(1')-C(2')	1.342(3)	N(1')-C(2')-C(7')	117.1(2)
C(2')-C(3')	1.366(4)	C(3')-C(2')-C(7')	125.1(2)
C(2')-C(7')	1.515(4)	C(2')-C(3')-C(4')	120.0(3)
O(1')-C(7')	1.256(3)	C(3')-C(4')-C(5')	121.2(3)
C(3')-C(4')	1.379(4)	C(6')-C(5')-C(4')	116.5(3)
O(2')-C(7')	1.228(3)	C(6')-C(5')-C(8')	121.2(3)
C(4')-C(5')	1.385(4)	C(4')-C(5')-C(8')	122.3(3)
C(11')-C(10')	1.247(9)	N(1')-C(6')-C(5')	120.9(3)
C(5')-C(6')	1.380(4)	O(2')-C(7')-O(1')	127.7(3)
C(5')-C(8')	1.500(4)	O(2')-C(7')-C(2')	117.4(3)
C(8')-C(9')	1.480(5)	O(1')-C(7')-C(2')	114.9(2)
C(9')-C(10')	1.598(7)	C(9')-C(8')-C(5')	114.5(3)
N(1)-C(2)-C(3)	121.5(3)	C(8')-C(9')-C(10')	111.1(4)
N(1)-C(2)-C(7)	118.5(3)	C(11')-C(10')-C(9')	120.0(7)
C(3)-C(2)-C(7)	119.9(3)		

Table 4-9. Anisotropic displacement parameters ($Å^2 x\ 10^3$) for NL2_0m. The anisotropic displacement factor exponent takes the form: $-2p^2[\ h^2\ a^{*2}U^{11} + ...\ + 2\ h\ k\ a^*\ b^*\ U^{12}\ ]$

	U^{11}	U^{22}	U^{33}	U^{23}	U^{13}	U^{12}
C(2)	66(2)	64(2)	86(2)	0(2)	-2(2)	1(1)
N(1)	93(2)	68(2)	122(2)	1(2)	-27(2)	-8(1)
O(1)	88(2)	61(1)	116(2)	4(1)	-30(1)	-6(1)
C(3)	82(2)	75(2)	131(3)	0(2)	-8(2)	10(2)
O(2)	104(2)	63(2)	165(2)	-17(2)	-28(2)	1(1)
C(4)	82(2)	106(3)	127(3)	7(2)	-17(2)	18(2)
C(11)	247(11)	570(20)	255(10)	-80(12)	12(9)	-220(14)
C(5)	72(2)	110(3)	102(2)	-12(2)	-7(2)	-5(2)
C(6)	102(3)	82(2)	141(3)	-8(2)	-28(3)	-13(2)
C(7)	77(2)	55(2)	96(2)	-3(2)	-1(2)	-1(2)
C(8)	91(3)	162(4)	120(3)	-21(3)	-14(2)	-14(3)
C(9)	93(3)	293(9)	211(5)	-99(6)	18(3)	-64(4)
C(10)	101(4)	426(15)	269(8)	-143(9)	27(5)	-108(6)
N(1')	69(2)	46(2)	76(2)	-3(1)	-6(1)	-2(1)
C(2')	70(2)	46(2)	72(2)	-2(1)	-5(1)	1(1)
O(1')	89(1)	53(1)	96(2)	-1(1)	-29(1)	-3(1)
C(3')	83(2)	50(2)	90(2)	2(1)	-11(2)	-4(1)
O(2')	102(2)	53(1)	104(2)	3(1)	-24(1)	10(1)
C(4')	79(2)	58(2)	96(2)	-4(2)	-13(2)	-9(2)
C(11')	144(6)	364(15)	357(13)	9(11)	-12(7)	54(7)
C(5')	70(2)	63(2)	79(2)	3(2)	-6(1)	1(2)
C(6')	70(2)	52(2)	81(2)	4(1)	-9(2)	2(1)
C(7')	82(2)	50(2)	79(2)	-3(1)	-7(2)	4(2)
C(8')	78(2)	82(2)	102(2)	8(2)	-18(2)	-3(2)
C(9')	77(2)	137(4)	155(4)	-1(3)	-2(2)	11(2)
C(10')	74(3)	118(4)	297(7)	-16(4)	7(4)	6(2)

Table 4-10. Hydrogen coordinates (x 10^4) and isotropic displacement parameters (Å^{2}x 10^3) for NL2_0m.

	x	y	z	U(eq)
H(1)	5226	2043	11301	156
H(3)	2143	3783	9545	128
H(4)	519	2999	8512	141
H(11A)	-3233	-12	8100	451
H(11B)	-3691	-584	7175	451
H(6)	1656	-494	9198	150
H(8A)	-260	1035	7562	164
H(8B)	75	-324	7965	164
H(9A)	-1393	1386	8368	248
H(9B)	-1068	16	8758	248
H(10)	-2083	-287	7067	329
H(1')	-1750(30)	1080(30)	2969(18)	85(9)
H(3')	-1038	4732	3213	101
H(4')	643	4254	4285	105
H(11C)	4873	1088	5168	467
H(11D)	5287	1694	6056	467
H(11E)	4800	2580	5277	467
H(6')	-152	533	3956	91
H(8'1)	1625	2620	5399	119
H(8'2)	1402	1160	5180	119
H(9'1)	2723	2752	4510	159
H(9'2)	2534	1273	4334	159
H(10A)	3665	2185	5986	212
H(10B)	3642	756	5707	212

*4.3 Glossary of NMR Terms**

COSY—COrrelation SpectroscopY—The COSY experiment determines proton-proton scalar coupling. This experiment produces a two-dimensional spectrum with both the axis and the ordinate labelled by the chemical shift of the observed nucleus (this nucleus is most often a proton). Cross peaks, or off-diagonal peaks, indicate the presence of scalar coupling between the two nuclei that correspond to those coordinates. The peaks along the diagonal reproduce the one-dimensional spectrum.

DEPT—Distortionless Enhancement by Polarization Transfer—A DEPT experiment allows for the identification of the degree of saturation of each carbon. This experiment involves the detection of proton magnetization and the subsequent transfer of this magnetization to the carbon it is directly coupled to. By altering the final proton pulse width, θ, various types of spin systems can be detected. A θ of 90° will produce a spectrum in which only methine carbons will appear. A θ of 135° will produce a spectrum in which methine and methyl carbons are positive while methylene carbons are negative. Quaternary carbons will never give a signal because polarization transfer is impossible. The tabulated ^{13}C data in this thesis contains data gleaned from the DEPT spectrum: *s* denotes no protons on a given carbon, *d* denotes one proton, *t* denotes two, and *q* denotes three.

HETCOR—HETeronuclear CORrelation spectroscopy—The HETCOR experiment detects proton-carbon scalar coupling and identifies individual proton-carbon attachments. This experiment is much like a COSY experiment except that one of the axes in the

resultant two-dimensional spectrum is now labelled by the carbon chemical shift while the other remains labelled by the hydrogen chemical shift.

HMQC—reverse detection on Heteronuclear Multiple Quantum Coherence Experiment—The HMQC experiment determines proton-carbon scalar coupling. This experiment involves carbon polarization transfer to hydrogen with observation of the proton signal. Delay, $1/2\pi J$, is set using a J value of approximately 140 Hz. This is the value of one-bond hydrogen-carbon scalar coupling interactions.

HMBC—multiple bond HMQC experiment—A type of HMQC experiment which detects long-range (multiple bond) proton-carbon coupling. The only parameter that differentiates HMBC from standard HMQC is the J value in HMBC of approximately 10 Hz. This allows the detection of scalar coupling between hydrogens and carbons that are two or three bonds apart and less, as opposed to the exclusively one-bond couplings detected by standard HMQC.

*Burton, R. A. Isolation and Structure Elucidation of Biologically Active Natural Products from Barringtonia Asiatica and Caesalipinia Brasilensis, BYU, Brigham Young University, 1998.

4.4 rDNA sequence of Fungus 6/35

```
   1 GTGCCAGCCGCCGCGGTAATTCCAGCTCCAATAGCGTATATTAAAGTTGT
  51 TGCAGTTAAAAAGCTCGTAGTTGAACCTTGGGCCTGGCTGGCCGGTCCGC
 101 CTCACCGCGTGCACTGGTTCGGCCGGGCCTTTCCCTCTGGGGAGCCCTAT
 151 GCCCTTCACTGGGTGTAGTGGGGAACCAGGACTTTTACTGTGAAAAAATT
 201 AGAGTGTTCAAAGCAGGCCTATGCTCGAATACATCAGCATGGAATAATAG
 251 AATAGGACGTGTGGTTCTATTTTGTTGGTTTCTAGGACCGCCGTAATGAT
 301 TAATAGGGACAGTCGGGGGCATCAGTATTCAATTGTCAGAGGTGAAATTC
 351 TTGGATTTATTGAAGACTAACTACTGCGAAAGCATTTGCCAAGGATGTTT
 401 TCATTAATCAGGAACGAAAGTTAGGGGATCGAAGACGATCAGATACCGTC
 451 GTAGTCTTAACCATAAACTATGCCGACTAGGGATCGGACGATGTTATTTT
 501 TTGACTCGTTCGGCACCTTACGAGAAATCAAAGTCTTTGGGTTCTGGGGGG
 551 AGTATGGTCGCAAGGCTGAAACTTAAAGAAATTGACGGAAGGGCACCAC
 601 CAGGAGTTAAAACAGACTTTACGGAAGACCGCAGTCTCTGCTCCTAAAAG
 651 CACAGCCTGTAATGGGTTGGTGGTACGCCTGATAAGTGTGCTAGTCGGGT
 701 GTTAACACGCCTGGCGACATCCTCAAATTGCGGGGAAGCCCTAAGTAAAAA
 751 GCAGCTACTACTAAGCGTGCCTTGAAAAAGAGCGCGTGGCAAAGCATAA
 801 CGGCTTTGGTACAGTAAAAACGTAGCGGCCTGGGGTAATCCGCAGCCAAG
 851 CTCCTAGTTAGACGGAGAAGGTTCAGAGACTTAACGGGGATGGGTAGGCC
 901 ACGGATATAGAAGGGCCTGCTTAAGATAAAGTCCATTGGCGGTATGAAAA
 951 TGCTACCTAAGTGCATCCTATAATAGGGAGCCTGCGGCTTAATTTGACTC
1001 AACACGGGGAAACTCACCAGGTCCAGACACAATGAGGATTGACAGATTGA
1051 GAGCTCTTTCTTGATTTTGTGGGTGGTGGTGCATGGCCGTTCTTAGTTGG
1101 TGGAGTGATTTGTCTGCTTAATTGCGATAACGAACGAGACATTTACCTGC
1151 TAAATAGCCCGTATTGCTTTGGCAGTACGCTGGCTTCTTAGAGGGACTAT
1201 CCGCTTAAGCGGGTGGAAGTTGGATGCAATAACAGGTCTGTGATGCCCTT
1251 AGATGTTCTGGGCCGCACGCGCGTTACACTGACAGAGACAGCGAGTACTT
1301 CCTTAGTAGAGATACTTGGGTAATCTTGTTAAACTCTGTCGTGCTGGGGA
1351 TAGAGCATTGCAATTATTGCTCTTCAACGAGGAATTCCTAGTAAGCGTAA
1401 GTCATCAACTTGCGTTGATTACGTCCCTGCCCTTTGTACACACCGCCCGT
```

4.5 rDNA Sequence of Fungus 11/17

```
  1 TGTACTGGTCCGGCCGGGCCTTTCCCTCTGTGGAACCCCATGCCCTTCAC
 51 TGGGTGTGGCGGGGAAACAGGACTTTTACTGTGAAAAAATTAGAGTGCTC
101 CAGGCAGGCCTATGCTCGAATACATTAGCATGGAATAATAGAATAGGACG
151 TGTGGTTCTATTTTGTTGGTTTCTAGGACCGCCGTAATGATTAATAGGGA
201 CAGTCGGGGGCATCAGTATTCAATTGTCAGAGGTGAAATTCTTGGATTTA
251 TTGAAGACTAACTACTGCGAAAGCATTTGCCAAGGATGTTTTCATTAATC
301 AGGAACGAAAGTTAGGGGATCGAAGACGATCAGATACCGTCGTAGTCTTA
351 ACCATAAACTATGCCGACTAGGGATCGGACGGTGTTATTTTTTGACCCGT
401 TCGGCACCTTACGAGAAATCAAAGTGCTTGGGCTCCAGGGGGAGTATGGT
451 CGCAAGGCTGAAACTTAAAGAAATTGACGGAAGGGCACCACCAGGGGTGG
501 AGCCTGCGGCTTAATTTGACTCAACACGGGGAAACTCACCAGGTCCAGAC
551 ACAATGAGGATTGACAGATTGAGAGCTCTTTCTTGATTTTGTGGGTGGTG
601 GTGCATGGCCGTTCTTAGTTGGTGGAGTGATTTGTCTGCTTAATTGCGAT
651 AACGAACGAGACCTTAACCTGCTAAATAGCCCGTATTGCTTTGGCAGTAC
701 GCTGGC
```